Efficient and Sustainable Reconfiguration of Distribution Networks via Metaheuristic Optimization

Postprint accepted for pubblication in *IEEE Transactions on Automation Science and Engineering*

How to cite: A. M. Helmi, R. Carli, M. Dotoli and H. S. Ramadan, (2021) "Efficient and Sustainable Reconfiguration of Distribution Networks via Metaheuristic Optimization," *IEEE Transactions on Automation Science and Engineering*. DOI: 10.1109/TASE.2021.3072862

Efficient and Sustainable Reconfiguration of Distribution Networks via Metaheuristic Optimization

Ahmed M. Helmi, Raffaele Carli, *Member, IEEE*,
Mariagrazia Dotoli, *Senior Member, IEEE*, and Haitham S. Ramadan, *Member, IEEE*

***Abstract*—Improving the efficiency and sustainability of distribution networks (DNs) is nowadays a challenging objective both for large networks and microgrids connected to the main grid. In this context, a crucial role is played by the so-called network reconfiguration problem, which aims at determining the optimal DN topology. This process is enabled by properly changing the close/open status of all available branch switches to form an admissible graph connecting network buses. The reconfiguration problem is typically modelled as an NP-hard combinatorial problem with a complex search space due to current and voltage constraints. Even though several metaheuristic algorithms have been used to obtain –without guarantees– the global optimal solution, searching for near–optimal solutions in reasonable time is still a research challenge for the DN reconfiguration problem. Facing this issue, this paper proposes a novel effective optimization framework for the reconfiguration problem of modern DNs. The objective of reconfiguration is minimizing the overall power losses while ensuring an enhanced DN voltage profile. A multiple-step resolution procedure is then presented, where the recent Harris Hawks optimization (HHO) algorithm constitutes the core part. This optimizer is here intelligently accompanied by appropriate pre-processing (i.e., search space preparation and initial feasible population generation) and post-processing (i.e., solution refinement) phases aimed at improving the search for near–optimal configurations. The effectiveness of the method is validated through numerical experiments on the IEEE 33–bus, the IEEE 85–bus systems, and an artificial 295–bus system under distributed generation and load variation. Finally, the performance of the proposed HHO-based approach is compared with two related metaheuristic techniques, namely the particle swarm optimization algorithm and the Cuckoo search algorithm. Results show that HHO outperforms the other two optimizers in terms of minimized power losses, enhanced voltage profile and running time.**

***Note to Practitioners*—This paper is motivated by the emerging need for effective network reconfiguration approaches in modern power distribution systems, including microgrids. The proposed metaheuristic optimization strategy allows the decision maker (i.e., the distribution system operator) to determine in reasonable time the optimal network topology, minimizing the overall power losses and considering the system operational requirements. The proposed optimization framework is generic and flexible, as it can be applied to different architectures both of large DNs and microgrids, considering various types of system objectives and technical constraints. The presented strategy can be implemented in any decision support system or engineering software for power grids, providing decision makers with an effective Information and Communication Technology tool for the optimal planning of the energy efficiency and environmental sustainability of DNs.**

***Index Terms*—Distribution Network Reconfiguration, Microgrids, Power Losses Reduction, Voltage Profile Improvement, Metaheuristic Optimization, Harris Hawks Optimization Algorithm.**

NOMENCLATURE

Acronyms

CSA	Cuckoo search algorithm
DN	distribution network
HHO	Harris hawks optimization
PSO	particle swarm optimization
SS	sectionalized switch
TS	tie switch

Set and Indices

$\mathcal{N}$	set of indices related to the nodes (buses) of the DN
$\mathcal{E}$	set of indices related to the branches (lines) of the DN
$\mathcal{G}$	graph representing the DN
$\mathcal{S}$	set of indices related to the switch-equipped branches
$\mathcal{S}_i$	set of indices related to the switch-equipped branches connected to bus i
$\mathcal{T}$	set of indices related to the branches with TS
j	index of branches with TS
i, k	indices of buses
$\mathcal{L}$	set of network loops

Parameters

N_{br}	number of switch-equipped branches
N_{bus}	number of buses
N_{gen}	number of generator nodes including the slack bus
N_{ts}	number of tie-switches
g_{ik}, b_{ik}	conductance and reactance of the line between buses i and k

Manuscript received on July 15, 2020; revised on November 4, 2020 and February 13, 2021; accepted April 3, 2021. (*Corresponding author: R. Carli.*)

The work of R. Carli and M. Dotoli is partially supported by Italian University and Research Ministry under project RAFAEL (National Research Program, contract n. ARS01-00305).

A. M. Helmi is with the Computer and Systems Department of the Zagazig University, Zagazig, Egypt and with the Engineering and Information Technology College, Buraydah Private Colleges, 51418 Buraydah, KSA (e-mail: amhm162@gmail.com).

R. Carli and M. Dotoli are with the Department of Electrical and Information Engineering of the Polytechnic of Bari, 70125 Bari, Italy (e-mail: {raffaele.carli, mariagrazia.dotoli}@poliba.it).

H. S. Ramadan is with the Electrical Power and Machines Department of the Zagazig University, 44519 Zagazig, Egypt, and with the ISTHY (Institut international sur le Stockage de l'Hydrogéne), 90400 Meroux-Moval, France (e-mail: haitham.s.ramadan@gmail.com).

V_{min}, V_{max}	voltage magnitude permissible limits
I_{max}	current magnitude maximum allowable limit
N_{pop}	size of initial population

Decision Variables

σ_j	status of the switch related to branch j
P^{loss}	overall power loss in the DN
P_j^{loss}	power loss at branch j of the DN
P_i, Q_i	real and reactive power at bus i
V_i, θ_i	voltage magnitude and angle at bus i
I_j	current magnitude in line j
$X_i^{(t)}$	network reconfiguration related to solution i and iteration step t
$c_i^{(t)}$	power loss of the network reconfiguration related to solution i and iteration step t
X_*	optimal network reconfiguration as computed by the HHO algorithm
c_*	power loss of the optimal network reconfiguration
$\tilde{X}_*$	optimal network reconfiguration as estimated by the refinement phase
$\tilde{c}_*$	power loss of the refined optimal network reconfiguration

I. Introduction

ELECTRICAL power Distribution Networks (DNs) are responsible for delivering power energy to many interconnected nodes. Consequently, improving the efficiency and sustainability of DNs is nowadays a challenging objective both for large networks and microgrids connected to the main grid [1], [2]. Differently from transmission networks, that are often based on a meshed structure, the topology of DNs is typically radial to reduce the short-circuit current. Nevertheless, DNs usually contain several branches connecting two nodes, or simply switches, making the resulting topology complex [3]. Throughout the DN, switches can be either normally–closed sectionalized switches (SSs) or normally–open tie–switches (TSs). By changing the close/open status of these switches, the so-called *DN reconfiguration* is performed, thus attaining different objectives, particularly power supply recovery and fault isolation [4]. Recently, obtaining automatically the most efficient DN reconfiguration through optimization tools has been considered among the due tasks for both reducing the network's real active power losses [5] and improving its voltage profile [6], as well as efficiently exploiting generators [7], optimally coordinating the distributed resources [8], satisfying load balancing [9] and congestion requirements [10], and in general improving the distribution system sustainability [11].

Fast expansions –either random or planned for– and complex structures of electrical power grids highlight the importance of different techno–economic objectives of DNs, such as: reliability of power supply [12], robustness of microgrid operations [13], grid security and resilience [14], and sustainable energy access [15]. Moreover, enhancing network structures in presence of distributed generation (DG) and distributed storage (DS) is gaining a particular interest for modern DNs, which more increasingly employ renewable sources and energy storage systems [16]. For the sake of achieving the optimal operation conditions, the selection of the optimal network configuration thus plays a crucial role.

Reconfiguration is a complex combinatorial problem, since multiple switches are involved with a number of configurations that exponentially grows as the system complexity and size increase [17]. As a consequence, the need for effective resolution methods for the DN reconfiguration problem is evident in the related literature. Even though several metaheuristic algorithms have been used to obtain –without guarantees– the global optimal solution, searching for near–optimal solutions in reasonable time is still a research challenge for the DN reconfiguration problem.

Facing this issue, this paper proposes a novel effective optimization framework for the reconfiguration problem of modern DNs. The objective of reconfiguration is minimizing the overall power losses, while ensuring an enhanced DN voltage profile. The DN graph is assumed to contain some loops –one for each deployed TS– which represent the search space of the optimization problem. The TSs are considered initially open and may be closed in accordance with the evolution of the reconfiguration process. A multiple-step reconfiguration resolution procedure is here presented, where the recent Harris Hawks optimization (HHO) algorithm constitutes the core part. This optimizer is here intelligently accompanied by appropriate pre-processing (i.e., search space preparation and initial feasible population generation) and post-processing (i.e., solution refinement) phases, aimed at improving the search for near–optimal configurations. The effectiveness of the method is validated through numerical experiments on the IEEE 33–bus and IEEE 85–bus systems – which are widely used by researchers as benchmarks for evaluating the performance of control solutions proposed in the power systems field – and an artificial 295-bus system under distributed generation and load variation. Finally, the performance of the proposed HHO-based approach is compared with two related well-known metaheuristic techniques, namely the particle swarm optimization (PSO) algorithm and the Cuckoo search algorithm (CSA) proposed in [18] and [19], respectively. Results show that HHO outperforms the other two optimizers in terms of minimized power losses, enhanced voltage profile and running time. More specifically, for the IEEE 33–bus, all the different optimizers successfully reached the near-optimal solution in all independent runs. For the larger IEEE 85–bus system and 295–bus system, HHO provides the highest performance in terms of minimized power losses and enhanced voltage profile, with the highest success rate and the lowest running time.

The rest of this paper is organized as follows: Section II sheds light on the state of the art related to the DN reconfiguration and positions the contribution of the paper. In Section III, the problem formulation is pointed out in terms of decision variables, objectives, and constraints. Moreover, Section IV is focused on the definition of the proposed resolution technique, describing in detail the algorithms to achieve the optimal DN reconfiguration. The results of numerical experiments are shown and discussed in Section V, including the performance comparison of the proposed optimization framework with

related methods. The conclusions and the future research directions are summarized in Section VI.

II. Related Works and Paper Contributions

Nowadays, research on the DN reconfiguration problem is attracting a notable consideration due to the growing advances in modern power generation, distribution technologies, and microgrids. Since the pioneering studies in the related literature [20], [21], the paradigm of tackling the reconfiguration problem is focused on closing initial TSs, identifying the meshes in the resulting graph, and opening a unique switch in each identified loop. Hence, the DN reconfiguration problem is framed into the NP-combinatorial optimization [17].

The the related literature in applied resolution techniques to solve this problem can be categorized into three classes: heuristic, metaheuristic, and artificial intelligence (AI) techniques. Heuristic methods like [20] and [21] have in common the disandvantage they might be trapped at local minima [5] and converge too early during the earch process, in particular in large-scale systems [18]. Conversely, AI techniques such as artificial neural networks [22] typically require extensive training examples in order to achieve reasonable success. To cope with these drawbacks, optimal DN reconfiguration studies recently rely on applying metaheuristic algorithms [23], [24]. On the one hand, single–solution based metaheuristic (also known as local search) approaches such as simulated annealing [25] and tabu search [6] find satisfying solutions by iteratively making small changes to the incumbent solution. On the other hand, different population–based metaheuristic methods such as firefly algorithm [5], cuckoo search [18], particle swam optimization [19], water cycle algorithm [26], genetic algorithms [27], fireworks algorithm [28], shuffled frog leaping algorithm [29], discrete artificial bee colony [30], harmonic search [31], ant colony [32], and hybrid big bang-big crunch algorithm [33] find good solutions by iteratively selecting and then combining existing solutions from a set, usually called the population. Nevertheless, reaching the global optimal solution is not yet guaranteed when metaheuristics approaches are employed. Consequently, obtaining near–optimal solutions in a reasonable time is still among the real research challenges.

Independently from the employed resolution techniques, the optimal DN reconfiguration problem commonly aims at minimizing power losses without violating the defined constraints [5], [18]–[33]. Some works focus on the optimization of further criteria related to the planning of power grids, e.g., maximizing the energy saving in presence of renewable energy sources [7], improving the loadability limit (i.e., the crititcal load that produces the voltage instability) of the DNs [34], reducing the voltage volatility induced by the deployed renewable energy sources [35], improving the reliability [36] and resilience of DNs [37] of the DNs, maximizing the network security [38]. The DN reconfiguration problem is also devoted to increasing the DS and DG penetration through the optimal placement and sizing of distributed generation (DG) [39] or distributed storage (DS) [40] and both of them [41]. Finally, in the area of power grid planning, the reconfiguration problem is subordinate to strategic decisions concerning the DN retrofit and maintenance. For instance, Raposo *et al.* [42] propose an optimization procedure based on genetic algorithms for the optimal placement of metering units in DNs with the final aim of accurately estimating the state of the grid under different configurations. Buhari *et al.* [43] introduce a method for selecting the most convenient DN configuration taking the cost-optimal replacement of cables into account.

From the review of the above mentioned works it follows that the majority of studies on DN reconfiguration focuses on planning purposes. Nevertheless, the optimal DN reconfiguration is often coupled with different problems addressed by the optimal operation of modern power systems, which typically include the penetration of renewable energy sources and the integration of energy storage solutions [44]. Several recent studies address the DN reconfiguration problem while evaluating the benefits resulting from the most convenient use and management of DG and DS. For instance, Iraji *et al.* [45] propose a PSO tool to define the optimal switch set topology for reconfigurable photovoltaic systems under both normal and abnormal conditions. Similarly, Li *et al.* [46] address the optimal operations of DNs in the presence of wind power by coordinating network reconfiguration. Conversely, Nick *et al.* [47] present an optimal control strategy for the management of the energy storage systems deployed in the network under different seasonal optimal configurations. The combined optimal management of both DG and DS in the reconfiguration problem is addressed in [48]. In addition, the optimal control of loads in the DNs can bring benefits to the network if well integrated in the reconfiguration process. For instance, Yang *et al.* [49] propose the comprehensive network reconfiguration and optimization of DNs using the coordination of flexible loads and TSs. Similarly, Andebili and Firuzabad [50] propose an adaptive approach for DN reconfiguration and charging management of plug–in electric vehicles. Shen *et al.* [51] propose a comprehensive scheme for day–ahead congestion management of DNs with high penetration of distributed energy resources. Liu *et al.* [52] show how the reconfiguration problem enhances the voltage regulation in unbalanced DNs. Mishra *et al.* [53] propose a restorative mechanism that automatically reconfigures the network taking the load priority into account.

Despite the rich state of the art on the optimal DN reconfiguration, very few research studies pay attention to crucial algorithmic aspects of the optimization problem. First, finding and extracting the main loops in the DN graph, when initial TSs are closed, in an efficient manner is mandatory in large–scale systems to reduce the effort in continuously preparing the search space. Second, repairing infeasible solutions, that is preparatory to obtaining adequate solutions, adds further complexity to the problem. Conversely, avoiding infeasible solutions should be preferred in the optimization in order to improve the effectiveness in reaching near–optimal solutions and reduce the execution time. Third, starting the optimization process on any random group of solutions, without preliminarily checking the constraints feasibility, may result in lower performance in terms of running time. Lastly, the problem constraints have to be properly addressed, since they significantly impact the solution research by bringing plenty

of local minima in the search space. To the best of the authors' knowledge, none of the cited works fully addresses all these mentioned issues simultaneously.

Differently from the above, this paper proposes a general optimization framework to effectively solve the DN configuration problem in a comprehensive and efficient fashion. In particular, a four-step procedure is presented, where the recent HHO algorithm – that constitutes the core part of the optimization framework – is intelligently accompanied by two pre-processing and a post-processing phases aimed at improving the search for near–optimal configurations. Upon the preparation of the used optimizer, and to enhance its effectiveness, the authors consider ignoring infeasible solutions in the initialization process and providing an efficient refinement procedure at the end of procedure. Thus, the search strategy is modified in order to overcome undesired local minima.

The contribution of this paper is thus fourfold and it is summarized as follows:

(i) employing the recent HHO algorithm with its four inherent searching strategies during the core part of the DN reconfiguration process. Differently from the state of the art, switching between these strategies during the update step minimizes the risks of reaching unacceptable local minima solutions;

(ii) implementing an efficient and different–scale–applicable robust metaheuristic offline algorithm for finding and extracting main loops in the DN graph. Differently from the existing works, the problem search space is prepared with minimal involvement of users;

(iii) proposing an appropriate generation of the initial population including feasible solutions only. This expedient allows to alleviate the amount of searching directions addressed by the core optimization process;

(iv) implementing an intelligent refinement procedure, that is adequate for the problem search space, to overcome the undesired time–consuming process of repairing infeasible solutions during optimization.

Finally, we highlight that the majority of the research works on DN reconfiguration validate the presented methods on test networks with a maximum of 136 buses [44]. For the sake of comprehensively testing the proposed HHO-based approach, we compare it with two other related metaheuristic techniques, namely the CSA and the PSO, both on the IEEE 33–bus, the IEEE 85–bus systems, and a large artificial 295-bus system equipped with distributed generation. The comparison analysis evaluates the perfomance of each optimizer in terms of minimized power losses, enhanced voltage profile and consumed running time.

III. Distribution Network Reconfiguration

A. System model

DNs are composed by several interconnected buses. Each bus can be connected to several components, such as loads or renewable energy sources. Moreover, DNs are connected to the transmission network through a slack bus, from which power is injected into the distribution grid. In this work we focus on single-phase DNs only. This assumption is not limiting, since multi-phase unbalanced networks can be converted into single-phase circuit models, so that methods for single-phase networks can be applied to the equivalent models of multi-phase unbalanced networks [54], [55].

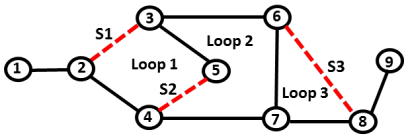

Figure 1. Example of a simplified DN with indication of the sectionalized–switches (solid line), tie–switches (dashed lines), and possible loops.

Let a generic DN be schematized by a number of N_{br} switch–equipped branches connecting a number of N_{bus} buses, as shown in the example of Fig. 1 where N_{bus}=9 and N_{br}=11. Initially, typically most of the switches are in the *close* status (SSs) (e.g., the branches in solid lines in Fig. 1), whilst the remaining ones are in the *open* status (TSs) (e.g., the branches in dashed lines in Fig. 1). Subsequently, each branch status can change according to the the desired topology through *switches*. Let us assume that the number of TSs and SSs in the DN is $N_{ts} \in \mathbb{N}_+$ and $(N_{br} - N_{ts}) \in \mathbb{N}_+$, respectively ($N_{ts}$=3 in Fig. 1).

Given the information about buses and branches, an undirected graph associated to the DN can be constructed. Let $\mathcal{G} = (\mathcal{N}, \mathcal{E})$ denote the corresponding DN graph, where $\mathcal{N}$ is the set of nodes (i.e., buses) with cardinality $|\mathcal{N}| = N_{bus}$, whilst $\mathcal{E} \in \mathcal{N} \times \mathcal{N}$ is the set of pairs of distinct nodes called edges. Specifically, node $i = 1$ identifies the slack bus. For the sake of keeping the notation light, instead of using the edge set $\mathcal{E}$, the graph is characterized by the set of N_{br} node pairs corresponding to the switch–equipped branches. Let $\mathcal{S} := \{1, \ldots, N_{br}\}$ uniquely denote the set of indices related to the DN branches. Considering that the DN branches include both initially–closed switches and initially–open ones, then the corresponding graph $\mathcal{G}$ presents a meshed structure. Specifically, it contains a number of loops equal to the number of TSs, i.e., N_{ts} (e.g., three loops exist in the network of Fig. 1 whereas threes TSs are defined).

The DN reconfiguration process consists in sweeping all the possible network topology by changing the status of some/all switches while aiming at achieving a specific objective. Note that a radial structure is usually preferred in DNs for reaching adequate operating conditions. In particular, the radial structure is maintained only if the network graph induced by the branches with closed switches is connected and contains no meshes. Thus, for any possible configuration, the following equality has to be verified:

$$N_{br} - N_{ts} = N_{bus} - 1. \tag{1}$$

Let $\sigma_j \in \{0, 1\}$ denote the status of the switch related to each branch $j \in \mathcal{S}$: $\sigma_j = 0$ means that the switch is open (i.e., it is a TS), viceversa $\sigma_j = 1$ means that the switch is closed (i.e., it is a SS). Any possible configuration of the given DN can be straightforwardly defined introducing the following set of branches that identify the position of TSs in the network:

$$\mathcal{T} := \{j \in \mathcal{S} \mid \sigma_j = 0\} \tag{2}$$

Hence, a possible configuration extracts a *tree* from graph $\mathcal{G}$ by merely defining the set $\mathcal{T} \subset \mathcal{S}$ whose cardinality is $|\mathcal{T}| = N_{ts}$.

B. Problem formulation

The DN reconfiguration problem consists in selecting the optimal combination of open/closed switches in order to optimize a given criterion. In this work, the main objective is minimizing the total active power losses and consequently improving the level of minimum voltages that may occur at buses. The overall power losses in the DN are expressed as:

$$P^{\text{loss}} = \sum_{j=1}^{N_{br}} \sigma_j P_j^{\text{loss}} \tag{3}$$

where P_j^{loss} denotes the power loss at branch j when the corresponding switch is closed. Assuming that branch $j \in \mathcal{S}$ connects the buses $i, k \in \mathcal{N}$, P_j^{loss} is then computed as [56]:

$$P_j^{\text{loss}} = g_j(V_i^2 + V_k^2 - 2V_iV_k\cos(\theta_i - \theta_k)),\ \forall j \in \mathcal{S} \tag{4}$$

where g_j is the line conductance of branch j, whilst V_i and θ_i denote respectively the voltage magnitude and angle at bus $i \in \mathcal{N}$. Note that V_i and θ_i can be determined solving the so-called power flow equations. Power flow is the well-known technique used to obtain the steady-state condition of electric power systems [57]. The power flow equations consist in balancing the real (P_i) and reactive (Q_i) power at each bus $i \in \mathcal{N}$:

$$\mathrm{P}_i = \sum_{j \in \mathcal{S}_i} \sigma_j P_j,\ \forall i \in \mathcal{N} \tag{5}$$

$$\mathrm{Q}_i = \sum_{j \in \mathcal{S}_i} \sigma_j Q_j,\ \forall i \in \mathcal{N} \tag{6}$$

where $\mathcal{S}_i \in \mathcal{S}$ represents the subset of branches connected to bus i and P_j and Q_j are defined as:

$$P_j = g_{ik}V_i^2 - V_iV_k(g_{ik}\cos(\theta_i - \theta_k) + b_{ik}\sin(\theta_i - \theta_k)), \forall j \in \mathcal{S} \tag{7}$$

$$Q_j = -b_{ik}V_i^2 - V_iV_k(g_{ik}\sin(\theta_i - \theta_k) - b_{ik}\cos(\theta_i - \theta_k)),\ \forall j \in \mathcal{S}. \tag{8}$$

In (7)-(8) parameters g_{ik} and b_{ik} coincide with the line conductance (g_j) and reactance (b_j) if buses i and k are connected by the branch j; instead, they are zero valued ($g_{ik} = b_{ik} = 0$) if buses i and k are not connected. Equations (5)-(6) allow to determine V_i and θ_i for each load bus and θ_i for each generator bus –except the slack bus– assuming that the value of the voltage magnitude and angle at the slack bus are known, the real active power and the voltage magnitude at each of the remaining $(N_{gen} - 1)$ generator buses, and the real and reactive power at each of the $(N_{bus} - N_{gen})$ load buses. Hence, the line current magnitude I_j in each branch j is computed as follows:

$$\begin{aligned} I_j &= \sqrt{(I_j^{\text{real}})^2 + (I_j^{\text{imag}})^2}, \\ I_j^{\text{real}} &= g_j(V_i\cos\theta_i - V_k\cos\theta_k) \\ &\quad - b_j(V_i\sin\theta_i - V_k\sin\theta_k), \\ I_j^{\text{imag}} &= g_j(V_i\sin\theta_i - V_k\sin\theta_k) \\ &\quad + b_j(V_i\cos\theta_i - V_k\cos\theta_k),\ \forall j \in \mathcal{S}. \end{aligned} \tag{9}$$

In addition to the power flow equations (5)-(6), the following constraints are considered in our optimal reconfiguration problem as in [4], [16]:

1) The magnitude voltage at any bus i should be within the predefined permissible limits V_{min} and V_{max} in order to maintain the delivered power quality:
$$V_{min} \le V_i \le V_{max}, \quad \forall i \in \mathcal{N} \setminus \{1\}. \tag{10}$$
2) The current flow in any branch j should not exceed the maximum allowable limit I_{max}:
$$\sigma_j I_j \le I_{max}, \quad \forall j \in \mathcal{S}. \tag{11}$$
3) The number of *open* switches chosen among the DNs branches has to be set equal to N_{ts} (i.e., number of TSs); equivalently, the number of *closed* switches has to be equal to the number of SSs:
$$\sum_{j=1}^{N_{br}} \sigma_j = N_{br} - N_{ts}. \tag{12}$$
Note that (12) does not guarantee the radial structure of the DN. To ensure such a condition, an appropriate search space preparation is preliminarily executed before solving the optimization problem (as described in the following section).

We remark that, since the main focus of the addressed reconfiguration problem lies in minimizing the power losses of the DN, in this work we assume that the power profiles of load and generator buses are scheduled: this means that all the loads are inflexible and all the generation units are non dispatchable (i.e., their power profile cannot be externally controlled by operators). Hence, no load and generator operational constraints (such as load dynamics or generator output power limit and ramping up/down bounding) are considered. As for the generators, however, this is not a restrictive assumption, since modern DNs typically employ renewable DG such as wind and solar systems.

Summing up, the optimal DN reconfiguration problem is formulated as follows:

$$\begin{aligned} &\min_{\{\mathcal{T} \subset \mathcal{S} \,|\, |\mathcal{T}| = N_{ts}\}} P^{\text{loss}} \\ &\text{s.t. } (5) - (6), (10) - (12). \end{aligned} \tag{13}$$

Finally, note that the DN reconfiguration problem (13) is a non-linear mixed integer programming (MINLP) problem that consists in determining the $(2N_{bus} - N_{gen} - 1)$ real variables related to the power flow and the N_{ts} integer variables related to the choice of the TS-equipped branches, under the $(2N_{bus} - N_{gen} - 1)$ power flow equations in (5)-(6), the $(2N_{bus} + N_{br})$ inequalities in (10) and (11) and the equality constraint in (12), in addition to the N_{ts} integrality conditions in (2).

IV. The Proposed Approach Based on Metaheuristic Optimization

We now propose a novel optimal network reconfiguration framework based on the four–step optimization procedure depicted in Fig. 2. The first step – described in detail in Algorithm 1 – consists in the search space preparation aimed

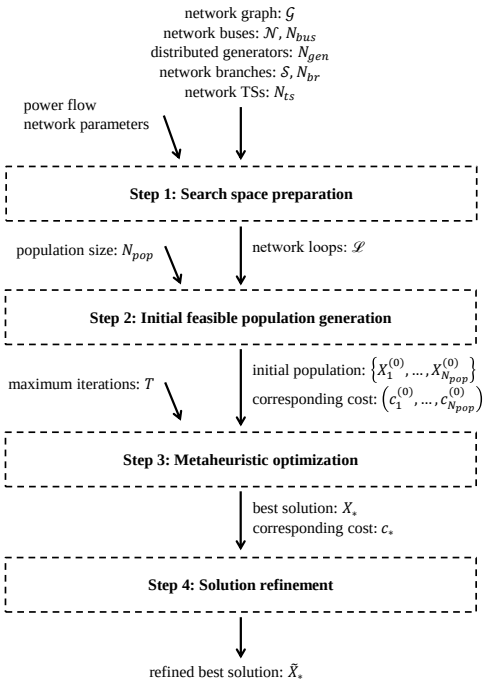

Figure 2. Scheme of the proposed optimal DN reconfiguration framework.

at extracting the loops from the induced network graph. The second step – described in detail in Algorithm 2 – is focused on the generation of the feasible initial population to be used in the metaheuristic optimization. As third step, the metaheuristic optimization is performed based on the recent four–stage HHO approach. The pseudo–code of the HHO procedure is illustrated in Algorithm 3. The fourth step aims at overcoming eventual local minima: hence, the solution obtained by the HHO optimizer is submitted to a refinement phase, as described in Algorithm 4.

A. Search Space Preparation

From an operational point of view, the radial feature of the DN has to be maintained through the reconfiguration process [18]–[22]. Both these features are available in the initial configuration thanks to the presence of N_{ts} open switches (i.e., TSs) and $(N_{br} - N_{ts})$ closed switches (i.e., SSs) among the DN branches. As previously mentioned, closing all the available TSs in the DN transform the network graph from a *tree* to a meshed graph $\mathcal{G}$ with a number of loops equal to the number of TSs (i.e., N_{ts}). A feasible alternative configuration to the initial one can be thus achieved by straightforwardly opening one switch per each loop of $\mathcal{G}$, so that the radiality and connectivity properties are both ensured. As a consequence, the set of loops in $\mathcal{G}$ form the problem search space.

The definition of the loops extraction procedure is reported in Algorithm 1 and is summarized in the sequel using the simplified DN depicted in Fig. 1 as an example.

As a precondition, all the TSs (i.e., (2,3), (4,5), and (6,8) in DN of Fig. 1) are supposed to get the close status; hence, the corresponding branches are part of the induced graph $\mathcal{G}$.

As a first step (Algorithm 1, line 2), the dangling nodes (i.e., 1 and 9 in DN of Fig. 1) and the corresponding edges are removed from $\mathcal{G}$. Note that at least one dangling node exists in real DNs: this coincides with the slack bus (i.e., bus 1 in the DN of Fig. 1) and its corresponding branch cannot be set as a TS. After removing the dangling nodes, the set of existing BCs of $\mathcal{G}$ contain all meshes.

The second step (Algorithm 1, line 3) consists in determining the set $\mathcal{B}$ of biconnected components (BCs) of $\mathcal{G}$ (i.e., $\{2, 3, 6, 7, 4\}$ and $\{6, 7, 8\}$ in the graph of Fig. 1). For instance, the depth–first search technique can be used to compute the BCs of $\mathcal{G}$. Note that a biconnected component is a maximal biconnected subgraph, i.e., a subgraph that is not properly contained in a larger biconnected subgraph (i.e., if and only if any node is deleted, the subgraph remains connected).

In the third step (Algorithm 1, line 4), the existing maximal BC β (i.e., $\{2, 3, 6, 8, 7, 4\}$ of the graph in Fig. 1) – that coincides to the graph exterior loop – is extracted from the set of BCs.

As a fourth step (Algorithm 1, lines 8-12) all the inner loops (i.e., $\{2, 3, 5, 4\}$ and $\{6, 7, 8\}$ of the graph in Fig. 1) are extracted in accordance with an iterative procedure, while ensuring all branches of $\mathcal{G}$ are reported at least in one loop.

As final step (Algorithm 1, line 14), all the branches duplicated in the extracted loops (i.e., $\{3, 5, 4, 7, 6\}$, $\{2, 3, 5, 4\}$ and $\{6, 7, 8\}$ of the graph in Fig. 1) are removed. This ensures that any branch in the final extracted loops can be TS only once. As a result, Algorithm 1 is a good-fit with the DN reconfiguration problem, since opening only a switch per loop successfully transforms the DN graph into a mesh–free spanning tree. In light of this observation, the definition of a DN configuration is coded as a vector $X := (X(1), \dots, X(k), \dots, X(N_{ts}))$ with N_{ts} integers. The k-th element of X identifies the branch belonging to loop k, which has to be set as a TS. A unique switch status modification is indeed allowed per each loop.

B. Initial Feasible Population Generation

High rates of reaching these infeasible solutions negatively impact both the execution time and solution quality. To avoid such an issue, an initial population of feasible solutions is generated to effectively determine the optimal reconfiguration in a time–saving fashion. Specifically, the procedure devoted to generate such a population of solutions is reported in Algorithm 2 and is summarized in the sequel.

Algorithm 2 is based on an iterative mechanism that is repeated until N_{pop} feasible solutions are identified (Algorithm 2, lines 2 and 10). Preliminarily, the population counter is initialized (Algorithm 2, line 1). The idea of the search mechanism basically relies on randomly opening one switch in each of the extracted loops (Algorithm 2, line 3). Then, the feasibility of the obtained corresponding network configuration is assessed by solving the power flow equations (Algorithm 2, line 4). If the network configuration is unfeasible or the power flow equations solver diverges, the corresponding candidate solution is discarded. Otherwise, the corresponding candidate solution is added to the initial population, the corresponding performance is stored, and the population counter is increased (Algorithm 2, lines 5-9).

Algorithm 1 Search Space Preparation

Inputs: $\mathcal{G}$

1: $k \leftarrow 1$
2: $\mathcal{G} \leftarrow$ remove dangling nodes in $\mathcal{G}$
3: $\mathcal{B} \leftarrow$ find biconnected components in $\mathcal{G}$
4: $\beta \leftarrow$ maximal component in $\mathcal{B}$
5: set all branches in $\mathcal{G}$ as unmarked
6: **while** at least one branch in $\mathcal{G}$ is unmarked **do**
7: $\quad j \leftarrow$ select an unmarked branch from β
8: $\quad \hat{\mathcal{G}} \leftarrow \mathcal{G} \setminus \{j\}$
9: $\quad \pi \leftarrow$ shortest–path between vertices of j in $\hat{\mathcal{G}}$
10: $\quad \mathcal{L}_k \leftarrow \{j, \pi\}$
11: $\quad$ mark j and all branches in π
12: $\quad k \leftarrow k + 1$
13: **end while**
14: remove any duplicated branches in the elements of $\mathcal{L}$

Outputs: $\mathcal{L}$

Algorithm 2 Initial Feasible Population Generation

Parameters: N_{pop}

Inputs: $\mathcal{L}$

1: $k \leftarrow 1$
2: **while** $k \leq N_{pop}$ **do**
3: $\quad X \leftarrow$ randomly open one switch per element of $\mathcal{L}$
4: $\quad$ c $\leftarrow P^{\text{loss}}(X)$ $\quad \triangleright$ *power flow resolution*
5: $\quad$ **if** $c < \infty$ **then**
6: $\quad\quad X_k^{(0)} \leftarrow X$
7: $\quad\quad c_k^{(0)} \leftarrow c$
8: $\quad\quad k \leftarrow k + 1$
9: $\quad$ **end if**
10: **end while**

Outputs: $\{X_1^{(0)}, \ldots, X_{N_{pop}}^{(0)}\}$, $(c_1^{(0)}, \ldots, c_{N_{pop}}^{(0)})$

We remark that the above described procedure identifies the initial feasible population by randomly selecting admissible solutions. This random selection does not induce any convergence issue as argued in the following. A candidate solution may have infinite losses (i.e., it is not admissible) either in the case of a disconnected DN graph or of a cyclic graph. Assuming that Algorithm 1 will terminate correctly, then the obtained loops contain all switches of the DN graph (both SSs and TSs) except for those that do not belong to some loop, like feeder bus and leaf buses (i.e., with degree 1). As a first consequence, disconnecting 1-degree buses is not possible. In addition, the set of reported loops are free of duplicated switches; hence, opening one switch is possible only in one loop. Since the number of TSs exactly equals to number of loops, then no cycle will exist DN graph after opening all the selected TSs.

Finally, it has to be noticed that the problem search space preparation, addressed by Algorithm 1, reduces significantly the generation rate of infeasible solutions by maintaining the radial structure of DNs, thus resulting in speeding up both Algorithm 2 and the subsequent optimization step.

C. Harris Hawks Optimization Algorithm

HHO is a recent population–based nature–inspired metaheuristic algorithm proposed in [58], which mimicks the hunting–behaviour of Harris-type hawks. These birds are cooperative predators that successfully perform harmonized foraging activities. During the hunting process, hawks cooperatively modify their attack–strategy considering the current position of the prey (e.g., a rabbit). A proper switching between different searching scenarios is taken into account to successfully hunt the prey. Similarly, the HHO algorithm aims at attaining the best solution in the search space while avoiding premature convergence to unsatisfactory points. This is the main advantage of this algorithm compared with other state-of-the art metaheuristic techniques [58]. In particular, the population of candidate solutions –representing the hawks positions– is updated throughout the algorithm processing until the best solution (i.e, the near optimum of the optimization problem) –representing the rabbit position– is achieved.

The HHO procedure is reported in Algorithm 3 and is summarized in the sequel. The algorithm is based on an iterative procedure: throughout this description the iteration step counter t is enclosed in the superscript of variables, whilst the maximum number of algorithm iterations is denoted as T. Preliminarly, the best solution is selected between the initial population (Algorithm 3, line 1). The iteration step counter is initialized (Algorithm 3, line 2) and the hunting mechanism is repeated until the termination criterion in satisfied (Algorithm 3, lines 3 and 29).

The HHO problem search space is mainly explored by each hawk (Algorithm 3, line 7) via two phases: exploration (Algorithm 3, lines 8-9) and exploitation (Algorithm 3, lines 10-25) [58]. The escaping energy of the rabbit, denoted by $E_i^{(t)}$, is the control parameter used by hawk i to transfer from exploration to exploitation at iteration t. $E_i^{(t)}$ is computed as follows (Algorithm 3, line 6):

$$E_i^{(t)} = (2r_{1,i}^{(t)} - 1)E_0^{(t)} \tag{14}$$

where $r_{1,i}^{(t)}$ is a time-varying random coefficient in the range $(0, 1)$ and $E_0^{(t)}$ is a diminishing stepsize (Algorithm 3, line 4):

$$E_0^{(t)} = 2\Big(1 - \frac{t}{T}\Big). \tag{15}$$

Note that (15) physically models the fact that the energy of a prey decreases considerably during the escape. The term $(2r_{1,i}^{(t)} - 1)$ in (14) takes values in $(-1, 1)$: the range $(0, 1)$ and $(-1, 0)$ means that the rabbit is physically strengthening and flagging, respectively, at iteration t.

During the exploration phase, hawks monitor the search space and are stationed in some locations in accordance with two perching strategies: (i) positions in the middle between the rabbit and other group members and (ii) random locations inside the group course of action [58]. Consequently, the candidate solution i is updated depending on the event probability

Algorithm 3 HHO algorithm

Parameters: T
Inputs: $\{X_1^{(0)},\ldots,X_{N_{pop}}^{(0)}\}$, $(c_1^{(0)},\ldots,c_{N_{pop}}^{(0)})$

1: $j = \text{argmin}_{i\in\{1,\ldots,N_{pop}\}}\, c_i^{(0)},\ X_* = X_j^{(0)}$
2: $t \leftarrow 0$
3: **while** $t < T$ **do**
4: update $E_0^{(t)}$ using (15) ▷ *diminishing stepsize*
5: **for each** $i := 1$ to N_{pop} **do**
6: update $E_i^{(t)}$ using (14) ▷ *escaping energy*
7: **if** $|E_i^{(t)}| \geq 1$ **then** ▷ *exploration*
8: update $X_i^{(t+1)}$ using (16)
9: **else** ▷ *exploitation*
10: $r_i^{(t)} \leftarrow \text{rand}(0,1)$
11: **if** $r_i^{(t)} \geq 0.5$ **then** ▷ *no rapid dives*
12: **if** $|E_i^{(t)}| \geq 0.5$ **then** ▷ *soft besiege*
13: update $X_i^{(t+1)}$ using (18)
14: **else** ▷ *hard besiege*
15: update $X_i^{(t+1)}$ using (21)
16: **end if**
17: **else** ▷ *rapid dives*
18: **if** $|E_i^{(t)}| \geq 0.5$ **then** ▷ *soft besiege*
19: update $X_i^{(t+1)}$ using (26)
20: **else** ▷ *hard besiege*
21: update $X_i^{(t+1)}$ using (27)
22: **end if**
23: **end if**
24: **end if**
25: $c_i^{(t+1)} \leftarrow P^{\text{loss}}([X_i^{(t+1)}])$ ▷ *power flow resolution*
26: **end for**
27: $j = \text{argmin}_{i\in\{1,\ldots,N_{pop}\}}\, c_i^{(t+1)},\ X_* = [X_j^{(t+1)}]$
28: $t \leftarrow t+1$
29: **end while**

Outputs: X_*

$q_i^{(t)}$ (randomly generated in $(0,1)$) as follows (Algorithm 3, line 8):

$$X_i^{(t+1)} = \begin{cases} X_* - \bar{X}_i^{(t)} - r_{2,i}^{(t)}(L + r_{3,i}^{(t)}(U-L)), & q_i^{(t)} < 0.5 \\ X_{\rho_i^{(t)}}^{(t)} - r_{4,i}^{(t)} \left| X_{\rho_i^{(t)}}^{(t)} - 2r_{5,i}^{(t)} X_i^{(t)} \right|, & q_i^{(t)} \geq 0.5 \end{cases} \tag{16}$$

where time-varying coefficients $r_{2,i}^{(t)}, r_{3,i}^{(t)}, r_{4,i}^{(t)}$, and $r_{5,i}^{(t)}$ are randomly generated in $(0,1)$, L and U are respectively the lower and upper bounds of solutions, $X_{\rho_i^{(t)}}^{(t)}$ is a randomly selected hawk in the current population (i.e., $\rho_i^{(t)}$ is the random integer in the range $[1, N_{pop}]$ selected by the hawk i at iteration t), and $\bar{X}_i^{(t)}$ is the average position of the current population estimated by the hawk i at iteration t:

$$\bar{X}_i^{(t)} = \sum_{j=1}^{N_{pop}} X_i^{(t)}. \tag{17}$$

As the search process proceeds, the escaping energy of the rabbit decreases. Thus, the exploitation phase of the hawks starts [58]. In this stage, four different intelligent strategies are considered for attacking the prey: soft or hard besiege, either without or with progressive rapid dives. The decision depends on the escaping energy level $E_i^{(t)}$ and the event probability $r_i^{(t)}$ randomly generated in $(0,1)$ (Algorithm 3, line 10).

For $r_i^{(t)} \geq 0.5$ and $|E_i^{(t)}| \geq 0.5$, each hawk i performs a soft besiege (Algorithm 3, lines 12-13). Since the prey still has enough energy for escaping by random misleading movements, the hawk softly encircles the rabbit with a surprise pounce–action. In this strategy, the candidate solution i is updated as follows:

$$X_i^{(t+1)} = \Delta X_i^{(t)} - E_i^{(t)} \left| J_i^{(t)} X_* - X_i^{(t)} \right| \tag{18}$$

where $\Delta X_i^{(t)}$ is the difference between the rabbit position and the current location of hawk i at iteration t:

$$\Delta X_i^{(t)} = X_* - X_i^{(t)} \tag{19}$$

and $J_i^{(t)}$ represents the strength of rabbit random movement throughout the escaping trial from hawk i at iteration t:

$$J_i^{(t)} = 2(1 - r_{5,i}^{(t)}) \tag{20}$$

where $r_{5,i}^{(t)}$ is a time-varying coefficient randomly chosen in $(0,1)$.

For $r_i^{(t)} \geq 0.5$ and $|E_i^{(t)}| < 0.5$, each hawk i performs a hard besiege (Algorithm 3, lines 14-16). Since the prey is too exhausted with inadequate escaping energy, the hawks hardly encircles the rabbit through a surprise pounce, thus performing a hard besiege. In this strategy, the candidate solution i is updated by:

$$X_i^{(t+1)} = X_* - E_i^{(t)} \left| \Delta X_i^{(t)} \right|. \tag{21}$$

For $r_i^{(t)} < 0.5$ and $|E_i^{(t)}| \geq 0.5$, each hawk i uses the soft besiege progressive rapid dives (Algorithm 3, lines 17-19). Since it is assumed that the rabbit tries escaping by using random movements, the hawks progressively select the best possible dive towards the prey comparing different movements, as actually found in real behavior. As a first option, each hawk i probes a smooth approach towards the rabbit:

$$Y_i^{(t)} = X_* - E_i^{(t)} \left| J_i^{(t)} X_* - X_i^{(t)} \right|. \tag{22}$$

As a second option, assuming that the rabbit reacts implementing a deceptive motion, each hawk i probes an abrupt and rapid dive towards the rabbit:

$$\hat{Y}_i^{(t)} = Y_i^{(t)} + \delta_i^{(t)}. \tag{23}$$

In (23) the term $\delta_i^{(t)}$ models the real zigzag of the pray [59] as follows:

$$\delta_i^{(t)} = s_i^{(t)} \circ \text{LF}_i^{(t)} \tag{24}$$

where $\circ$ denotes the entry-wise product, $s_i^{(t)}$ is a N-dimensional time-varying vector of random coefficients in $(0,1)$, and $\text{LF}_i^{(t)}$ is a N-dimensional vector of levy flight coefficients. Note that $\text{LF}_i^{(t)}$ is computed as follows [59]:

$$\text{LF}_i^{(t)} = \frac{\psi\, u_i^{(t)}}{\left| v_i^{(t)} \right|^{\frac{1}{\beta}}}, \psi = \left(\frac{\Gamma(1+\beta)\, sin(\frac{\pi\beta}{2})}{\Gamma(\frac{1+\beta}{2})\, \beta\, 2^{(\frac{\beta-1}{2})}} \right)^{\frac{1}{\beta}} \tag{25}$$

where $u_i^{(t)}$ is a N-dimensional time-varying vector of random coefficients in $(0,1)$, $v_i^{(t)}$ is a time-varying random coefficients in $(0,1)$, $\Gamma(\cdot)$ is the gamma function, and β is a default constant set to 1.5. The final strategy is thus selected as the best performing between the previous movement $X_i^{(t)}$ and the current options (22) and (23):

$$X_i^{(t+1)} = \begin{cases} Y_i^{(t)}, & \text{if } P_{loss}([Y_i^{(t)}]) < P_{loss}(X_i^{(t)}) \\ \hat{Y}_i^{(t)}, & \text{if } P_{loss}([Y_i^{(t)}]) \geq P_{loss}(X_i^{(t)}) \wedge \\ & P_{loss}([\hat{Y}_i^{(t)}]) < P_{loss}(X_i^{(t)}) \\ X_i^{(t)}, & \text{elsewhere} \end{cases} \quad (26)$$

For $r_i^{(t)} < 0.5$ and $|E_i^{(t)}| < 0.5$, each hawk i uses the hard besiege progressive rapid dives (Algorithm 3, lines 20-24). Similarly to the standard hard besiege, hawks aim at decreasing the distance between their average location and the rabbit location. In this strategy, the rule for updating the candidate solution i is the following:

$$X_i^{(t+1)} = \begin{cases} Z_i^{(t)}, & \text{if } P_{loss}([Z_i^{(t)}]) < P_{loss}(X_i^{(t)}) \\ \hat{Z}_i^{(t)}, & \text{if } P_{loss}([Z_i^{(t)}]) \geq P_{loss}(X_i^{(t)}) \wedge \\ & P_{loss}([\hat{Z}_i^{(t)}]) < P_{loss}(X_i^{(t)}) \\ X_i^{(t)}, & \text{elsewhere} \end{cases} \quad (27)$$

where $Z_i^{(t)}$ and $\hat{Z}_i^{(t)}$ respectively denote the smooth and the abrupt movements, determined as follows:

$$Z_i^{(t)} = X_* - E_i^{(t)} \left| J_i^{(t)} X_* - \bar{X}_i^{(t)} \right| \quad (28)$$

$$\hat{Z}_i^{(t)} = Z_i^{(t)} + \delta_i^{(t)} \quad (29)$$

using the average position of hawks $\bar{X}_i^{(t)}$ computed in (17), the rabbit strength determined in (20), and the time-varying coefficient $\delta_i^{(t)}$ defined in (24).

At the end of each iteration, the cost of each solution in the updated population is calculated, the new best solution is identified, and the iteration counter is incremented (Algorithm 3, lines 25-28). Note that metaheuristic optimizers are originally employed for defining real–valued solutions in continuous optimization problems. However, the DN reconfiguration solution requires integer values (i.e., the identifiers of TSs in the DN constructed graph). To this aim, a rounding procedure is used to obtain the adequately coded configuration before evaluating the corresponding performance (i.e., the overall power losses of the corresponding DN configuration) through the power flow equations resolution (Algorithm 3, lines 25). Since the loops extracted by Algorithm 1 are free of duplications, the candidate solutions obtained by the rounding procedure are mesh–free, thus preserving the required radial structure of the given network. Infeasible solutions may only result from divergences of the Newton–Raphson method employed by the power flow solver.

D. Solution Refinement

After the optimizer achieves the best solution, a final refinement trial is performed. The execution of such a refinement allows verifying whether the achieved solution actually is a near–optimal solution that outperforms any other DN configuration. This local search is performed by the fast and greedy procedure described in in Algorithm 4.

Algorithm 4 Solution Refinement

Inputs: X_*, N_{ts}, $\mathcal{L}$

1: $\tilde{X}_* \leftarrow X_*$, $\tilde{c}_* \leftarrow c_*$
2: **for** $k := 1$ to N_{ts} **do**
3: $\quad X \leftarrow \tilde{X}_*$
4: $\quad \lambda \leftarrow \mathcal{L}_k$
5: $\quad$ **for** $j := 1$ to $|\lambda|$ **do**
6: $\quad\quad X(k) \leftarrow \lambda(j)$
7: $\quad\quad c \leftarrow P^{\text{loss}}(X)$ ▷ *power flow resolution*
8: $\quad\quad$ **if** $c < \tilde{c}_*$ **then**
9: $\quad\quad\quad \tilde{X}_* \leftarrow X$, $\tilde{c}_* \leftarrow c$
10: $\quad\quad$ **end if**
11: $\quad$ **end for**
12: **end for**

Outputs: $\tilde{X}_*$

The basic idea of Algorithm 4 is to replace some of the opened switches in the obtained solution with many others to obtain the minimum level of the overall power losses. To this aim, Algorithm 4 mainly evaluates the contribution that the *open* status of each switch in each extracted DN loop separately could provide in obtaining the optimal configuration, while fixing the status of all other switches. Two nested iteration loops are thus employed: the outer *for* loop (Algorithm 4, line 2) scans all the elements in the set $\mathcal{L}$ of DN Loops, whilst the inner *for* loop (Algorithm 4, line 5) analyzes all the branches in a single loop. In each iteration the analyzed switch is set to *open* status, while all the remaining switches in the same loop are kept in the *close* status: a new DN configuration is thus obtained (Algorithm 4, line 6). The feasibility and the performance of this new DN configuration are evaluated (Algorithm 4, line 7) by solving the power flow equations. If the results outperform the current solution, the latter is replaced by the new DN configuration (Algorithm 4, line 9). Note that each DN branch is considered just once during the execution of the entire refinement procedure, implying that the total number of power flow solver callings (Algorithm 4, line 7) is always less than the number N_{br} of DN branches.

V. Numerical Experiments Results and Analysis

A. Simulations Setup

The proposed optimal network reconfiguration framework is validated through numerical experiments based on: (i) the IEEE 33–bus system, (ii) the IEEE 85–bus system, and (iii) an artificial 295–bus system equipped with DG.

The IEEE 33–bus system is a small-scale distribution system with 33 buses, where 5 TSs are added to the 32 distribution lines (each equipped with a SS) for a total of 37 branches as shown in Fig. 3.a. This DN shows 5 loops if all the switches take the *close* status. The line parameters and locations of the initial TSs related to the 33–bus system are inferred from [4], [5] and they are listed in Table I.

(a) IEEE 33–bus system

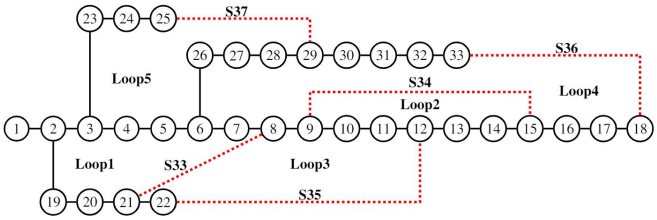

(b) IEEE 85–bus system

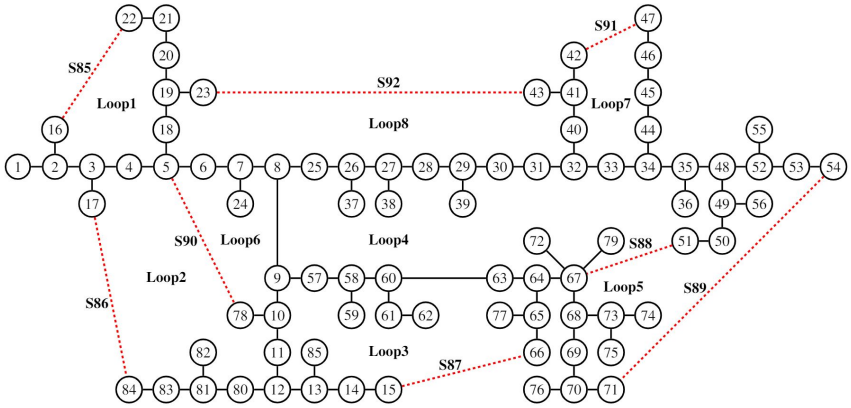

(c) 295–bus system with distributed generation

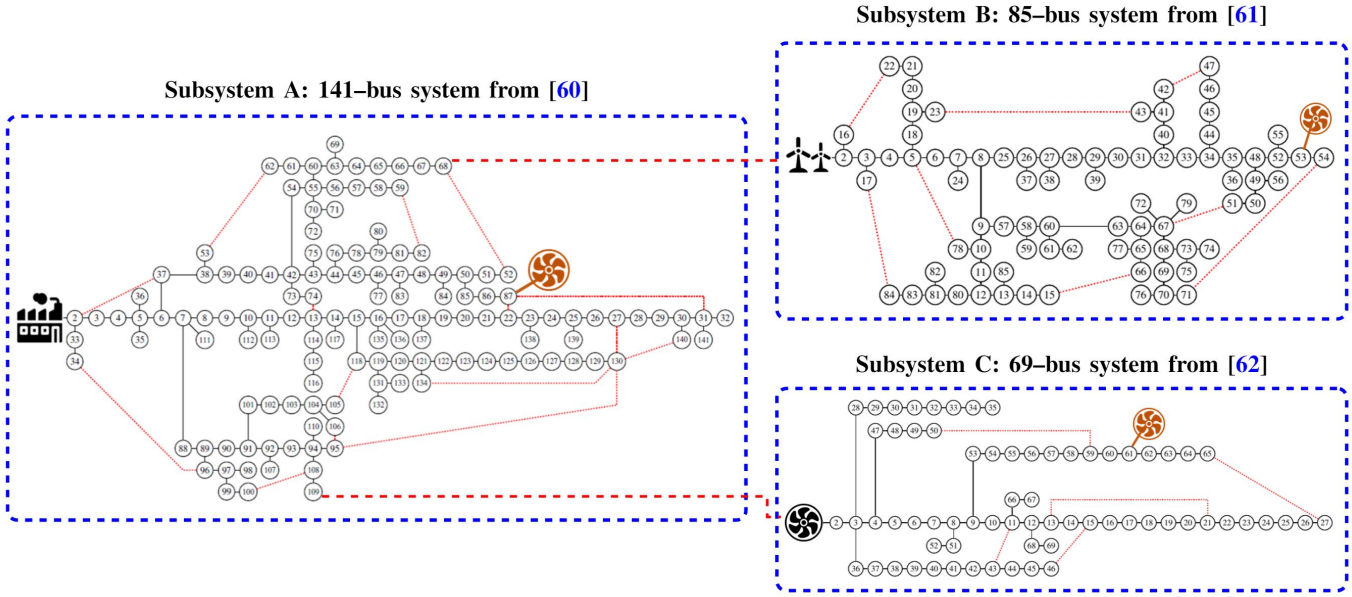

Figure 3. Initial configuration of the analyzed DNs with indication of the sectionalized–switches (solid line), tie–switches (dashed lines), and possible loops.

The IEEE 85–bus system [61] is a DN with 85 buses, which are connected through 92 branches (84 distribution lines equipped with SSs and 8 TSs) as shown in Fig. 3.b. By closing all the switches, 8 loops appear in the graph of this network. The initial TS parameters are presented in Table II: resistance (r_j) and reactance (x_j) data are selected on a similar basis to those for the 119–bus system addressed by [6]. In particular, the average ratio between r_j and x_j is approximately set to 2.28.

The 295–bus system is an artificial large DN composed by

Table I
LINE PARAMETERS FOR THE TS-EQUIPPED BRANCHES IN THE INITIAL CONFIGURATION OF THE IEEE 33-BUS SYSTEM.

branch j	connected buses (i,k)	resistance r_j [Ω]	reactance x_j [Ω]
33	(21, 8)	1.248	1.248
34	(9, 15)	1.248	1.248
35	(12, 22)	1.248	1.248
36	(18, 33)	0.312	0.312
37	(25, 29)	0.312	0.312

Table II
LINE PARAMETERS FOR THE TS-EQUIPPED BRANCHES IN THE INITIAL CONFIGURATION OF THE IEEE 85-BUS SYSTEM.

branch j	connected buses (i,k)	resistance r_j [Ω]	reactance x_j [Ω]
85	(16, 22)	0.53	0.29
86	(17, 84)	0.35	0.12
87	(15, 66)	0.5	0.25
88	(51, 67)	0.49	0.17
89	(54, 71)	0.39	0.14
90	(5, 78)	0.65	0.23
91	(42, 47)	0.68	0.25
92	(43, 23)	0.46	0.16

Table III
LINE PARAMETERS FOR THE TS-EQUIPPED BRANCHES IN THE INITIAL CONFIGURATION OF THE 295-BUS SYSTEM.

sub–system	branch j	connected buses (i,k)	resistance r_j[Ω]	reactance x_j[Ω]
141–bus	141	(53,62)	0.0280	0.0198
	142	(34,96)	0.0651	0.0471
	143	(2,37)	0.0265	0.0352
	144	(13,74)	0.0570	0.0404
	145	(22,87)	0.1222	0.0866
	146	(130,140)	0.1946	0.0476
	147	(59,82)	0.1231	0.0871
	148	(52,68)	0.1347	0.0953
	149	(130,134)	0.1552	0.1098
	150	(105,118)	0.0487	0.0345
	151	(100,108)	0.0878	0.0639
	152	(95,106)	0.0446	0.0315
	153	(95,130)	0.0118	0.0084
	154	(31,87)	0.0751	0.0532
	155	(27,130)	0.1505	0.0367
85–bus	85	(16,22)	0.53	0.29
	86	(17,84)	0.35	0.12
	87	(15,66)	0.5	0.25
	88	(51,67)	0.49	0.17
	89	(54,71)	0.39	0.14
	90	(5,78)	0.65	0.23
	91	(42,47)	0.68	0.25
	92	(43,23)	0.46	0.16
69–bus	69	(27,69)	0.599	0.253
	70	(46,52)	0.3855	0.1274
	71	(15,50)	0.2628	0.1869
	72	(35,27)	0.3215	0.1619
	73	(65,67)	0.5235	0.1757

the three DNs proposed in [60], [61], and [62], representing the sub–system A, B, and C shown in Fig. 3.c, respectively. Sub–system A is equipped with a diesel generator with a 10 MW capacity, and it has 141 buses, 140 distribution lines with SSs, and 15 TSs, for a total of 155 branches. Sub–system B is the IEEE–85 bus considered in case (ii). This sub–system is equipped with a wind turbine (denoted as WT) with a capacity of 12 MW, whose generation level varies between 0.68 and 1 following the daily profile in [64] shown on an hourly basis in Fig. 4.a. Sub–system C has 69 buses, 68 distribution lines equipped with SSs, and 5 TSs, for a total of 73 branches. This sub–system is equipped with a micro-turbine (denoted as $MT1$) with a capacity of 11.6 MW, whose generation starts after in the second part of the day and reaches its peak value in the late evening [65], as reported in the hourly-based profile profile of Fig. 4.b. The whole 295–bus system is obtained by connecting the generator of sub–systems B and C respectively to bus 68 and 109 of sub–system A via two ad-hoc TSs (shown in heavy dashed red lines in Fig. 3.c). We assume that these two TSs, which can be used to drive the sub–systems in islanded mode of operation, are forced to be in the *closed* status (i.e., they do not appear in any loop of the 295–bus system graph), leaving the 295–bus system equipped with distributed generation throughout the reconfiguration process. Summing up, the 295–bus system contains 322 distribution lines in total, where 294 branches are initially equipped with SSs and 28 with TSs. This DN shows 28 loops if all the switches take the *close* status. All the line parameters and the initial locations of TSs are presented in Table III. In particular, the line parameters of sub–system B are those considered in case (ii), whilst the line parameters of sub–system C are inferred from [62]. As for sub–system A, the DN proposed in [60] is modified by randomly replacing 15 distribution lines with TS-equipped branches: the corresponding values of r_j and x_j are multiplied by a factor equal to 20. Conversely, the line parameters of the remaining branches (i.e., the lines equipped with SSs) are obtained multiplying the values reported in [60] by a factor equal to 100. Furthermore, for the sake of highlighting the DN reconfiguration features in presence of distributed generation, three additional micro-turbines (denoted as $MT2$) are connected to the buses 87, 194, and 287, as indicated by the orange icons in Fig. 3.c. In particular, $MT2$ has a capacity of 5.8 MW and a generation level varying between 0.25 and 0.5 p.u. as shown in Fig. 4.b. Finally, a time-varying demand is considered in the 295–bus system. In all the load buses both the active and reactive power are assumed to follow the load variation profile $l(h)$ shown on a hourly basis in Fig. 4.d, with $h \in [1, 24]$. The active power at load bus i at the h-th time slot is determined as $P_i(h) = \bar{P}_i(1 + l(h))$, where $\bar{P}_i$ is the daily averaged active power load at load bus i shown in Fig. 4.c. The daily reactive power profile at load buses is determined similarly.

For all the above described DNs, a comparison of the results achieved by the proposed optimization procedure using three different optimizers is performed in accordance with the evaluation metrics described in the sequel. In particular, the HHO defined in Algorithm 3 is compared with the well-known CSA and the PSO algorithm proposed in [18] and [19], respectively. For the PSO implementation, in this work the cost function and PSO settings are defined according to [19]. Conversely, for the CSA implementation, the typical values for the search parameters are chosen: namely, the discovery rate is set to 0.25, the distribution factor is equal to $2/3$ and the step size is 0.01.

For all the three described optimizers, the inputs are obtained through the execution of the preliminary phases (namely, the search space preparation and the population initialization). The final result of each optimizer is subsequently processed by the last phase, i.e., the solution refinement. Given the stochastic nature of these optimizers, an accurate assessment of their behaviour requires the analysis of several runs. Consequently, the obtained values of the total power losses and the minimum voltage are calculated in terms of average and standard deviation. In addition, to ensure a fair–qualitative

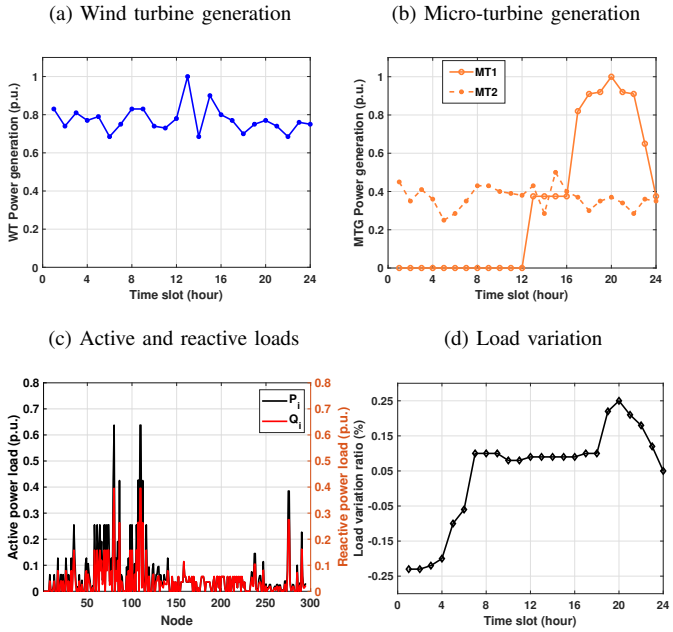

Figure 4. Generators and loads setup for the 295–system.

and quantitative evaluation, the population size, the maximum number of iterations, and the number of runs (considering same initial population in every run) are respectively set to 30, 100, and 20 for each optimizer.

Aside from the total power losses and the minimum voltage, the following further evaluation indices are considered in the comparison analysis: *1) Reduction ratio* for the losses $P^{\text{loss,r}}$ after reconfiguration with respect to the losses $P^{\text{loss,i}}$ related to the initial configuration, defined as $1 - P^{\text{loss,r}}/P^{\text{loss,i}}$; *2) Success rate* in obtaining the best–solutions, which is defined as the ratio between the number of runs where the best solution is found and the total number of runs; *3) Running time* incurred on average by the whole optimization procedure and by the individual optimizer over the given runs.

Finally, it is to be noticed that the proposed optimization procedure including the three analyzed optimizers is implemented in Matlab R2019, while all the simulations are run on a desktop PC with a 2.60 GHz CPU and 8 GB RAM. As for the resolution of the power flow equations, the Matpower package [63] is used under the Matlab environment.

B. Results Analysis and Discussion

33–bus system. For the initial configuration the total amount of real power losses is equal to 208.46 kW whilst the minimum voltage is 0.9107 p.u. (achieved at bus 18).

Solving the reconfiguration problem for such a relatively simple system with a limited number of switches, the different optimizers PSO, CSA and HHO achieve almost similar performance. In particular, it is evident from Table IV that the use of the refinement step does not provide significant improvement to any of the three optmizers. From Table IV, after the refinement step, the best solution is attained with the set of TSs equal to {7, 9, 14, 32, 37}: the corresponding optimal value of power losses and minimum voltage is 138.93

Table IV
SIMULATION RESULTS FOR THE IEEE 33–BUS SCENARIO.

		PSO		CSA		HHO	
		Av.	Std.	Av.	Std.	Av.	Std.
Optimizer	Losses (kW)	139.29	0.37	138.96	0.16	139	0.22
	Reduction (%)	33.18	0.18	33.34	0.07	33.32	0.11
	Min. Volt (p.u.)	0.9423	0	0.9423	0	0.9423	0
Refinement	Losses (kW)	138.93	0	138.93	0	138.93	0
	Reduction (%)	33.35	0	33.35	0	33.35	0
	Min. Volt (p.u.)	0.9423	0	0.9423	0	0.9423	0
Best Solution	Losses (kW)	138.93					
	Reduction (%)	33.35					
	Min. Volt (p.u.)	0.9423					
	TS branches	7, 9, 14, 32, 37					
	TS buses	(7,8), (9,10), (14,15), (32,33), (25,29)					
Success Rate (%)		100		100		100	
Time (s)	Initialization	0.3					
	Optimizer	9.5		20		17	
	Refinement	1.8					
	Total	11.6		22.1		19.1	
Init. Config.	Losses (kW)	208.46					
	Min. Volt (p.u.)	0.9107					
MINLP results	Losses (kW)	136.57					
	Time	647.0					

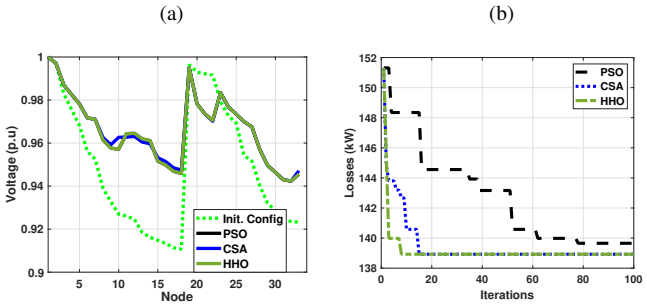

Figure 5. Average voltage profiles (a) and convergence curves (b) for the IEEE 33–bus system.

kW and 0.9423, respectively. Note that the success rate is 100% for all optimizers. The voltage profile achieved in Fig. 5.a shows that the behaviour of all three optimizers is very similar on average. As for the running time, the initialization (i.e., phases 1 and 2) and the solution refinement (i.e., phase 4) are executed in 0.3 s and 1.8 s, respectively. The average single full–run of PSO, CSA, and HHO lasts about 11.6 s, 22.1 s, and 19.1 s, respectively. The HHO thus outperforms the other optimizers in convergence speed, as also shown From Fig. 5.b. From the results in Table IV, it is apparent that, although the PSO is faster and the CSA has a lower standard deviation, the HHO algorithm is the best optimizer considering both rapidity and standard deviation in addition to the success rate. Nevertheless, in such a relative–small scale DN, the superiority of the HHO remains unclear compared to other optimizers.

Finally, we remark that solving the IEEE 33–bus system reconfiguration problem by a MINLP solver (e.g., the branch and bound technique proposed in [66]) leads to the same results obtained by our approach in terms of power losses but at the cost of a higher computational burden. As shown in the last two rows of Table IV, the optimality gap for the HHO is 1.8% while the execution time required branch and bound technique is around 34 times higher, as reported in [66].

85–bus system. For the initial configuration the total

Table V
SIMULATION RESULTS FOR THE IEEE 85–BUS SCENARIO.

		PSO		CSA		HHO	
		Av.	Std.	Av.	Std.	Av.	Std.
Optimizer	Losses(kW)	214.53	6.11	196.29	2.46	193.87	2.95
	Reduction (%)	32.14	1.93	37.91	0.78	38.67	0.93
	Min. Volt (p.u.)	0.8885	0.0106	0.9116	0.0049	0.9109	0.0038
Refinement	Losses(kW)	196.48	6.64	191.71	1.75	190.77	0.68
	Reduction (%)	37.85	2.1	39.36	0.55	39.65	0.22
	Min. Volt (p.u.)	0.9075	0.0125	0.9149	0.0029	0.9152	0.0026
Best Solution	Losses(kW)	190.56					
	Reduction (%)	39.72					
	Min. Volt (p.u.)	0.9165					
	TS branches	9, 11, 19, 31, 44, 53, 64, 88					
	TS buses	(9,10), (11,12), (19,20), (31,32), (44,45), (53,54), (64,65), (51,67)					
Success Rate (%)		5		45		75	
Time (s)	Initialization	16					
	Optimizer	35		49		40	
	Refinement	7.5					
	Total	58.5		72.5		63.5	
Init. Config.	Losses(kW)	316.14					
	Min. Volt (p.u.)	0.8713					

(a) (b)

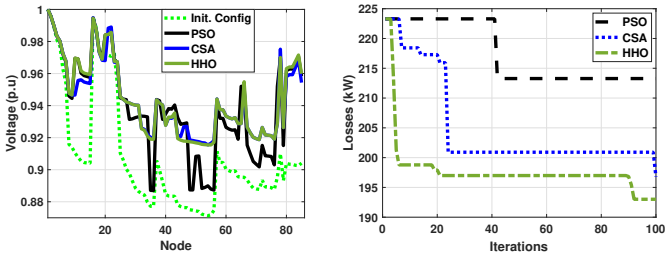

Figure 6. Average voltage profiles (a) and convergence curves (b) for the IEEE 85–bus system.

amount of real power losses is 316.14 kW, whilst the value of the minimum voltage is 0.8713 p.u. (achieved at bus 54).

From the results collected in Table V, it is evident that the HHO reports on average the best results among the three optimizers over the given runs before applying the solution refinement. The average value of losses is 193.87 kW with standard deviation of 2.95 kW. Thus, the reduction ratio of losses is 38.67% (standard deviation 0.93%). Moreover, the minimum voltage gets 0.9109 p.u. with standard deviation 0.0038. In second place, the CSA achieves a slightly lower performance. In comparison with both HHO and CSA, the worst results are obtained by the PSO. Figure 6.a reports the average solution for all the optimizers from the perspective of the bus voltage profile, showing that the HHO approach clearly provides better improvements than the PSO and CSA in all the buses. After applying the refinement procedure, further enhancements are reached for the PSO results, which get closer to those of the CSA. However, the HHO results keep the first ranking with a reduction ratio equal to 39.65% and a minimum voltage of 0.9152 p.u. Despite the very close results attained by the HHO and CSA techniques, the better robustness and reliability of the HHO approach over CSA are apparent, as demonstrated by its smaller standard deviation value and higher success rate. The standard deviation values are 0.68 kW and 0.0026 p.u. for losses and minimum voltage respectively. The near–optimal results of 190.56 kW losses and 0.9165 minimum voltage, corresponding to the set of TSs

Table VI
SIMULATION RESULTS OF THE LOAD VARIATION ANALYSIS FOR THE IEEE 85–BUS SYSTEM.

Scenario			Init. Config. → Reconfig.
Losses (kW)	1.18 × PQ		462.77 → 277.28
Loss Red. (%)			40
MinV (p.u.)			0.8439 → 0.9008
Solution (TS)		Bus	9 ,10 ,19 ,31 ,43 ,48 ,64 ,70
		Line	(9,10) ,(10,11) ,(19,20) ,(31,32), (34,44) ,(48,49) ,(64,65) ,(70,71)
Losses (kW)	0.8 × PQ		192.27 → 120.9
Loss Red. (%)			37.12
MinV (p.u.)			0.89983 → 0.93491
Solution (TS)		Bus	10 ,19 ,31 ,43 ,48 ,65 ,70 ,77
		Line	(10,11) ,(19,20) ,(31,32) ,(34,44), (48,49) ,(65,66) ,(70,71) ,(10,78)

(a) initial configuration (b) reconfiguration

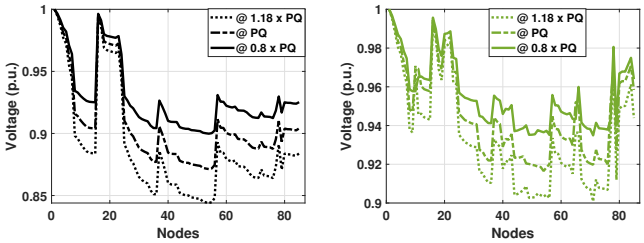

Figure 7. Voltage profile over nodes in the IEEE 85–bus system, for different load variation scenarios.

{9, 11, 19, 31, 44, 53, 64, 88}, are obtained in 15 out of 20 (i.e., 75%) independent runs. The success rates for the CSA and PSO are 45% and 5%, respectively. As for the running time, the initialization and the solution refinement procedures last 16 s and 7.5 s, respectively. The execution of the PSO, HHO and CSA optimizer requires 58.5 s, 63.5 s, and 72.5 s, respectively. Similarly to the IEEE 33–bus scenario, from Fig. 6.b it is evident that the HHO outperforms the other optimizers in terms of convergence speed.

Finally, for the sake of assessing the behavior of the proposed method under active and reactive power load variations, we report the analysis of the DN reconfiguration under load mitigation/elevation. In particular, we consider two scenarios of load variation within the addressed DN. In the first scenario, 80% of active and reactive power loads are applied to the 85–bus system. In the second scenario, both active and reactive power are increased by 18% over their nominal values. Table VI presents the results of the HHO approach, where losses are reduced by more than 37%, and minimum voltage magnitude is above 0.9 p.u. in both scenarios. Figure 7 shows the voltage profile for different load scenarios, before and after applying the proposed approach. From these results, it is evident that the HHO approach is successful in achieving reasonable solutions under under load variations; hence, the robustness is ensured for critical situations like load elevation.

295–bus system. First, for the sake of assessing the results of the HHO approch under a generation and load time-varying scenario, the DN reconfiguration problem is solved through the proposed method on an hourly basis using the daily production and demand profiles shown in Fig. 4. As a reference for the entire simulation period, the initial configuration corresponding to the TSs indicated in Table VII is used:

(a) power losses reduction (b) daily average voltage profile

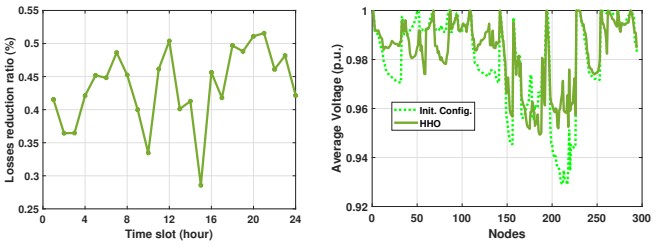

Figure 8. Results of the generation and load variation analysis for the 295–bus system.

(a) (b)

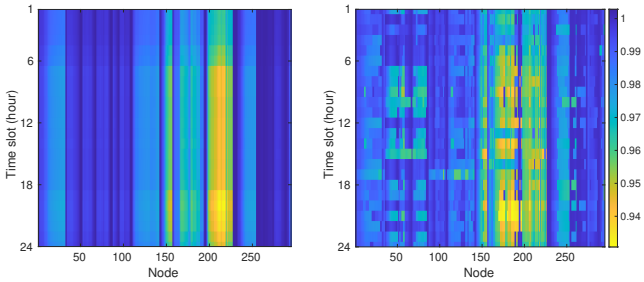

Figure 9. Initial (a) and optimally reconfigured (b) daily voltage profile (p.u.) for the 295–bus system under generation and load variation.

in such a configuration the overall power losses is equal to 2988.5 kW in average along 24 hours, with minimum voltage magnitude equal to 0.9292 p.u. in average along 24 hours. Figure 8.a reports the reduction ratio of the losses (ranging from 28% up to 51.5%) over the analyzed time slots in the whole 295–bus system, showing the notable effectiveness of the proposed HHO approach in minimizing the power losses in large DNs in presence of distributed generation. Initial power losses ranges from 1249.5 kW at 1h (lowest load demand) to 4555.6 kW at 22h (close to peak load). However, losses are successfully reduced to 766 kW at 1h and 2455.6 kW at 22h. In addition, Fig. 8.b emphasizes the enhanced voltage profile at each bus averaged along 24 hours after applying the proposed HHO approach. In the initial configuration the minimum voltage magnitude occurs at bus 217 with value of 0.913 p.u. at the time slot h =20 (load demand peak), whilst in the reconfigured system the bus 186 has in average the lowest voltage magnitude equal to 0.9307 p.u. at the time slot $h = 21$. The detailed daily voltage profile is presented in Fig. 9 for the best reconfiguration found by the proposed HHO approach.

Subsequently, to compare the performance obtained by the HHO approach on the 295–bus system with those achieved by the PSO and CSA techniques, a detailed analysis related to a given instant, namely the time slot $h = 20$, is reported in the sequel. As shown in Table VII, the HHO algorithm achieves a reconfiguration solution with losses equal to 2310.4 kW on average, with a reduction ratio equal 48.2%. Conversely, the CSA and PSO algorithms lead to worse results, since their reduction ratios are equal to 35.3% and 34%, respectively. The standard deviation for all three optimizers is relatively large compared to the 33-bus and 85-bus system scenarios. This proves the notable search complexity of the 295–bus system.

Table VII
SIMULATION RESULTS FOR THE 295–BUS SYSTEM AT TIME SLOT $h = 20$.

		PSO		CSA		HHO	
		Av.	Std.	Av.	Std.	Av.	Std.
Optimizer	Losses(kW)	2888.6	445	2951.9	299	2310.4	136
	Reduction (%)	35.3	10	34	7	48.2	3
	Min. Volt (p.u.)	0.9237	0.006	0.9130	0	0.9305	0.0075
Refinement	Losses(kW)	2588.6	413	2900.7	351	2184.6	137.8
	Reduction (%)	42	9.2	35	7.8	51.1	3
	Min. Volt (p.u.)	0.9292	0.0048	0.9150	0.0061	0.9318	0.0069
Best Solution	Losses(kW)	1950.2					
	Reduction (%)	56.34					
	Min. Volt (p.u.)	0.9360					
	TS branches	13, 15, 26, 34, 38, 59, 61, 101, 107, 120, 124, 141, 151, 152, 161, 172, 187, 189, 194, 206, 237, 251, 259, 271, 287, 299, 302, 309 (11,12), (13,14), (24,25), (2,33), (6,37), (57,58), (55,60), (99,100),					
	TS buses	(104,106),(118,119),(122,123),(30,140),(150,151),(151,152),(160,161), (171,172), (186,187),(176,189),(193,194),(205,206),(237,238), (251,252),(259,260),(271,272),(287,288),(22,87), (52,68),(27,130)					
Success Rate (%)		0		0		40	
Time (sec)	Initialization			160			
	Optimizer	83.1		139		89.6	
	Refinement			19			
	Total	262.1		318		268.6	
Init. Config.	Losses(kW)	4467.5					
	Min. Volt (p.u.)	0.9130					

We remark that, before applying the refinement procedure, the HHO approach is successful in achieving the minimum voltage equal to 0.9305 p.u., which is higher than the value of 0.9237 p.u. and 0.9130 p.u. achieved respectively by the CSA and PSO methods. Figure 10.a reports the average solution for all the optimizers from the perspective of the bus voltage profile, showing that the HHO approach clearly provides better improvements than the PSO and CSA in all the buses. In addition, from Table VII it is evident that the use of the refinement step provides significant improvement to all three optimizers, proving that the crucial importance of the proposed refinement procedure in large and distributed DNs. The refined solution achieved by the HHO approach is characterized by power losses equal to 2184.6 kW (i.e., the reduction ratio is 51.1%), with a standard deviation of 137.8 kW, and minimum voltage equal to 0.9318 p.u.. Even though the refinement procedure enhances the solutions obtained by the PSO and CSA algorithms, the achieved results are lower than those obtained by HHO: as for PSO the power losses reduction ratio is 42.0%, with a standard deviation of 413 kWh, and minimum voltage is 0.9292 p.u., whilst the losses reduction ratio, the standard deviation, and the minimum voltage achieved by the CSA algorithm are respectively equal to 35.0%, 351 kWh, and 0.9150 p.u.. Moreover, we remark that, differently from the PSO and CSA, the HHO approach is able to find solutions close to the best solution (the locations of TSs branches in the best solution are reported in Table VII), whose corresponding power losses and minimum voltage are respectively equal to 1950.2 kW and of 0.9360 p.u.. This property is ensured by the considerably high success rate of the HHO algorithm which is equal to 40%; in contrast, neither the CSA nor PSO algorithms are able to find the best solution in at least one run (i.e., the success rate is 0). As for the running time, the initialization and the solution refinement procedures last 160 s and 19 s, respectively. The execution of the PSO, CSA, and HHO optimizer takes 83.1 s, 139 s, and 89.6 s, respectively. Similarly to the previous scenarios, from Fig. 10.b it is evident

that the HHO outperforms the other optimizers in terms of convergence speed.

Finally, Fig. 11 summarizes the performance of the optimizers for the 295–bus scenario: it is clear that the HHO provides the best compromise for all the discussed evaluation metrics (the lowest losses, the highest success rate, an acceptable execution time) with respect to the other two tested techniques. Summing up, the results achieved by the refined HHO are promising under different settings, especially for large-scale DNs.

VI. Conclusions and Perspectives

This study addresses the problem of distribution networks (DNs) reconfiguration, which is vital to enhance the quality of power distribution systems. A multiple-step resolution procedure is proposed, where the Harris Hawks optimization (HHO) algorithm constitutes the core part, accompanied by appropriate pre- and post-processing phases aimed at improving the search for near-optimal configurations. The comparison with two related metaheuristic techniques shows that the HHO approach can be conveniently used for large–scale problems in acceptable execution time. However, forthcoming researches will address the reconfiguration problem in harder scenarios as well as in presence of uncertain generation and/or load variations, line outage and contingencies.

This study is not without limitations, which still need to be investigated in future works. In particular, the main limitation of the proposed framework relies on the use a mono-objective function. Due to techno-economic reasons, the resolution of the reconfiguration problem may be preferably performed under multiple objectives. Therefore, future work will mainly be devoted to defining a multi-objective approach to simultaneously address related problems, such as the optimal placement/sizing of distributed generators and storage systems, the congestion management, the improvement of network reliability and resilience, as well as the optimal energy scheduling of controllable loads and dispatchable generators connected to the addressed DN.

Moreover, the power grids addressed by the proposed model are single-phase. Since DNs are notoriously multi-phase and unbalanced, future research will be focused on extending the reconfiguration problem resolution taking the multi-phase unbalanced power flow into account. Finally, one may observe that results and implications are derived from a static scenario in an offline setting. Actually, this limitation is only apparent, since the proposed approach converges in a reasonable execution time and thus it can be easily incorporated in a receding horizon mechanism for real-time reconfiguration of the distribution grid. This aspect will be the subject of future research.

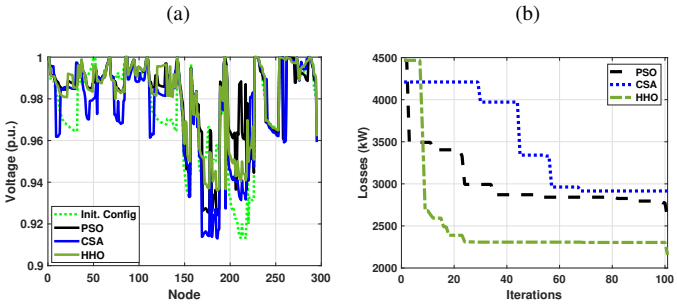

Figure 10. Average voltage profiles (a) and convergence curves (b) for the 295–bus system at time slot $h = 20$.

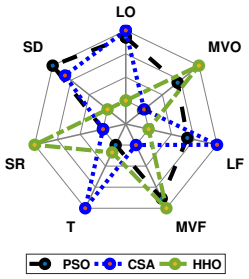

Figure 11. Radar plot of the results achieved by the 295–bus system at time slot $h = 20$. Metrics of evaluation are: average losses of solutions of optimizer and final solution after refinement *LO* and *LF*, respectively, average minimum voltage of solutions of optimizer and final solution *MVO* and *MVF*, respectively, standard deviation of final solutions *SD*, success rate *SR* and total execution time *T*. Data are normalized with respect to the highest value.

References

[1] Z. Yang, L. Xia and X. Guan, "Fluctuation Reduction of Wind Power and Sizing of Battery Energy Storage Systems in Microgrids," *IEEE Trans. Autom. Sci. Eng.*, 17(3), 1195-1207, 2020.

[2] R. Minciardi and M. Robba, "A Bilevel Approach for the Stochastic Optimal Operation of Interconnected Microgrids," *IEEE Trans. Autom. Sci. Eng.*, 14(2), 482-493, 2017.

[3] S. Babaei, R. Jiang and C. Zhao, "Distributionally Robust Distribution Network Configuration Under Random Contingency," *IEEE Trans. Power Syst.*, 35(5), 2020.

[4] A. Anderos, S. Koziel and M. F. Abdel-Fattah, Distribution network reconfiguration using feasibility–preserving evolutionary optimization, *J. Mod. Power Syst. Clean Energy*, 7, 589–598, 2019.

[5] M. A. Samman, H. Mokhlis, N. N. Mansor, H. Mohamad, H. Suyono and N. M. Sapari, Fast Optimal Network Reconfiguration With Guided Initialization Based on a Simplified Network Approach, *IEEE Access*, 8, 11948-11963, 2020.

[6] D. Zhang, Z. Fu, L. Zhang. An improved TS algorithm for loss-minimum reconfiguration in large-scale distribution systems, *ELECTR POW SYST RES*, 77(5–6), 685–694, 2007.

[7] V. B. Pamshetti, S. Singh and S. P. Singh, "Combined Impact of Network Reconfiguration and Volt-VAR Control Devices on Energy Savings in the Presence of Distributed Generation," *IEEE Syst. J.*, 14(1), 995-1006, 2020.

[8] D. Wu, T. Yang, A. A. Stoorvogel and J. Stoustrup, "Distributed Optimal Coordination for Distributed Energy Resources in Power Systems," *IEEE Trans. Autom. Sci. Eng.*, 14(2), 414-424, 2017.

[9] P. Gangwar, A. Mallick, S. Chakrabarti and S. N. Singh, "Short-Term Forecasting-Based Network Reconfiguration for Unbalanced Distribution Systems With Distributed Generators," *IEEE Trans. Ind. Inform.*, 16(7), 4378-4389, 2020.

[10] D. B. Nguyen, J. M. A. Scherpen and F. Bliek, "Distributed Optimal Control of Smart Electricity Grids With Congestion Management," *IEEE Trans. Autom. Sci. Eng.*, 14(2), 494-504, 2017.

[11] Gutiérrez-Alcaraz, G., Galván, E., González-Cabrera, N., and Javadi, M. S. (2015). Renewable energy resources short-term scheduling and dynamic network reconfiguration for sustainable energy consumption. *RENEW SUST ENERG REV*, 52, 256-264.

[12] Z. Li, W. Wu, B. Zhang and X. Tai, "Analytical Reliability Assessment Method for Complex Distribution Networks Considering Post-Fault Network Reconfiguration," *IEEE Trans. Power Syst.*, vol. 35, no. 2, pp. 1457-1467, 2020.

[13] S. M. Hosseini, R. Carli and M. Dotoli, "Robust Optimal Energy Management of a Residential Microgrid Under Uncertainties on Demand

and Renewable Power Generation," *IEEE Trans. Autom. Sci. Eng.*, doi: 10.1109/TASE.2020.2986269.

[14] H. Khazraj, B. Y. Khanghah, P. Ghimire, F. Martin, M. Ghomi, F. Faria da Silva and C. L. Bak, Optimal operational scheduling and reconfiguration coordination in smart grids for extreme weather condition, *IET Generation, Transmission & Distribution*, 13(15), 3455-3463, 2019.

[15] P. Ciller, S. Lumbreras, Electricity for all: The contribution of large-scale planning tools to the energy-access problem, *RENEW SUST ENERG REV*, 120, 109624, 2020.

[16] N. C. Koutsoukis, D. O. Siagkas, P. S. Georgilakis and N. D. Hatziargyriou, "Online Reconfiguration of Active Distribution Networks for Maximum Integration of Distributed Generation," *IEEE Trans. Autom. Sci. Eng.*, vol. 14, no. 2, pp. 437-448, 2017.

[17] S. Mohamed, M. F. Shaaban, M. Ismail, E. Serpedin and K. A. Qaraqe, "An Efficient Planning Algorithm for Hybrid Remote Microgrids," *IEEE Trans. Sustain. Energy*, 10(1), 257-267, 2019.

[18] T. T. Nguyen, A. V. Truong, Distribution network reconfiguration for power loss minimization and voltage profile improvement using cuckoo search algorithm, *INT J ELEC POWER*, 68, 233–242, 2015.

[19] A. Tandon and D. Saxena, A comparative analysis of SPSO and BPSO for power loss minimization in distribution system using network reconfiguration, *2014 Innovative Applications of Computational Intelligence on Power, Energy and Controls with their impact on Humanity (CIPECH)*, Ghaziabad, 226–232, 2014

[20] Merlin A, Back H. Search for a minimal loss operating spanning tree configuration in an urban power distribution system. *Proc. 5th Power System Computation Conf. (PSCC)*, Cambridge (UK), 1975. pp. 1–18.

[21] Civanlar S, Grainger JJ, Le SSH. Distribution feeder reconfiguration for loss reduction. *IEEE Trans. Power Deliv.*, 3(3), 1217-1223, 1988.

[22] Qiu R, Lv X, Chen S. A Survey on Artificial Intelligence Algorithm for Distribution Network Reconfiguration. *LECT NOTES CONTR INF.* Springer. 2011. p. 497–504.

[23] Badran, O., Mekhilef, S., Mokhlis, H., and Dahalan, W. (2017). Optimal reconfiguration of distribution system connected with distributed generations: A review of different methodologies. *Renew. Sust. Energ. Rev.*, 73, 854-867.

[24] Thakar, S., Vijay, A. S., and Doolla, S. (2019). System reconfiguration in microgrids. *Sustainable Energy, Grids and Networks, 17, 100191*.

[25] Jeon, Y. J., Kim, J. C., Kim, J. O., Shin, J. R., & Lee, K. Y. "An efficient simulated annealing algorithm for network reconfiguration in large-scale distribution systems," *IEEE Trans. Power Del.*, 17(4), 1070-1078, 2002.

[26] M. A. Muhammad, H. Mokhlis, K. Naidu, A. Amin, J. F. Franco and M. Othman, "Distribution Network Planning Enhancement via Network Reconfiguration and DG Integration Using Dataset Approach and Water Cycle Algorithm," *J MOD POWER SYST CLE*, 8(1), 86-93, 2020.

[27] K. Prasad, R. Ranjan, N. C. Sahoo, and A. Chaturvedi, Optimal configuration of radial distribution systems using a fuzzy mutated genetic algorithm, *IEEE Trans. Power Del.*, 20(2), 1211-1213, 2005.

[28] Imran, A.M., Kowsalya, M. A new power system reconfiguration scheme for power loss minimization and voltage profile enhancement using Fireworks Algorithm. *Electr Power Syst Res*, 62, 312–322, 2014.

[29] Arandian, B, Hooshmand, R.A., Gholipour, E. Decreasing activity cost of a distribution system company by reconfiguration and power generation control of DGs based on shuffled frog leaping algorithm. *Electr Power Energy Syst*, 61, 48–55, 2014.

[30] Aman MM, Jamson GB, Bakar AHA, Mokhilis H. Optimum network reconfiguration based on maximization of system load ability using continuation power flow theorem. *Electr Power Energy Syst*, 54, 123–133, 2014.

[31] Srinivasa Rao R, Ravindra K, Satisk K, Narasimham SVL. Power loss minimization in distribution system using network reconfiguration in the presence of distributed generation. *IEEE Trans. Power Syst.* 28(1), 317–325, 2013.

[32] Swarnkar Anil, Gupta Nikhil, Niazi KR. Adapted ant colony optimization for efficient reconfiguration of balanced and unbalanced distribution systems for loss minimization. *Swarm Evol Comput*, 1(3), 129–137, 2011.

[33] Sedighizadeh, M., Esmaili, M., Esmaeili, M. Application of the hybrid Big Bang-Big Crunch algorithm to optimal reconfiguration and distributed generation power allocation in distribution systems. *Energy*, 76, 920–930, 2014.

[34] A. Tyagi, A. Verma and P.R Bijwe, Reconfiguration for loadability limit enhancement of distribution systems, *IET Generation, Transmission & Distribution*, 12, 88-93, 2017.

[35] Y. Song, Y. Zheng, T. Liu, S. Lei and D. J. Hill, "A New Formulation of Distribution Network Reconfiguration for Reducing the Voltage Volatility Induced by Distributed Generation," *IEEE Trans. Power Syst.*, 35(1), 496-507, 2020.

[36] Z. Li, W. Wu, X. Tai and B. Zhang, "Optimization Model-based Reliability Assessment for Distribution Networks Considering Detailed Placement of Circuit Breakers and Switches," *IEEE Trans. Power Syst.*, 35(5), 3991-4004, 2020.

[37] J. Liu, Y. Yu and C. Qin, Unified two-stage reconfiguration method for resilience enhancement of distribution systems, *IET Generation, Transmission & Distribution*, 13, 1734-1745, 2019.

[38] G. Zu, J. Xiao and K. Sun, Distribution network reconfiguration comprehensively considering N–1 security and network loss, *IET Generation, Transmission & Distribution*, 12, 1721-1728, 2018.

[39] Z. Gong, Q. Chen and K. Sun, Novel methodology solving distribution network reconfiguration with DG placement, *The Journal of Engineering IET*, 2019(16), 1668-1674, 2019.

[40] W. Han and L. Zhang, Battery cell reconfiguration to expedite charge equalization in series-connected battery systems, *IEEE Robot. Autom. Lett.*, 3(1), 22-28, 2018.

[41] A. Azizivahed et al., "Energy Management Strategy in Dynamic Distribution Network Reconfiguration Considering Renewable Energy Resources and Storage," *IEEE Trans. Sustain. Energy*, 11(2), 662-673, 2020.

[42] Raposo, A. A., Rodrigues, A. B., da Silva, M. D. G. Robust meter placement for state estimation considering distribution network reconfiguration for annual energy loss reduction. *ELECTR POW SYST RES*, 182, 106233, 2020.

[43] M. Buhari, V. Levi and A. Kapetanaki, Cable replacement considering optimal wind integration and network reconfiguration, *IEEE Trans. Smart Grids*, 9(6), 5752-5763, 2018.

[44] Sultana, B., Mustafa, M. W., Sultana, U., and Bhatti, A. R. (2016). Review on reliability improvement and power loss reduction in distribution system via network reconfiguration. *Renew. Sust. Energ. Rev.*, 66, 297-310.

[45] F. Iraji, E. Farjah and T. Ghanbari, Optimization method to find the best switch set topology for reconfiguration of photovoltaic panels, *IET Renewable Power Generation*, 12, 374-379, 2018.

[46] Z. Li, S. Wang, Y. Zhou, W. Liu, X. Zheng, Optimal distribution systems operation in the presence of wind power by coordinating network reconfiguration and demand response, *INT J ELEC POWER*, 119, 2020.

[47] M. Nick, R. Cherkaoui and M. Paolone, Optimal planning of distributed energy storage systems in active distribution networks embedding grid reconfiguration, *IEEE Trans. Power Syst.*, 33(2), 1577-1590, 2018.

[48] Raul Vitor Arantes Monteiro, Jakson Paulo Bonaldo, Raoni Florentino da Silva, Arturo Suman Bretas, Electric distribution network reconfiguration optimized for PV distributed generation and energy storage, *ELECTR POW SYST RES*, 184, 2020.

[49] Y. Yang, S. Zhang, W. Pei, J. Sun and Y. Lu, Network reconfiguration and operation optimization of distribution system with flexible DC device, *The Journal of Engineering IET*, 2019(16), 2401-2404, 2019.

[50] M. R. Andebili and M. F. Firuzabad , Adaptive approach for PEVs charging management and reconfiguration of electrical distribution system penetrated by renewables, *IEEE Trans. Ind. Informat.*, 14(5), 2001-2010, 2018.

[51] F. Shen, S. Huang, Q. Wu, S. Repo, Y. Xu, and J. østergaard, Comprehensive congestion management for distribution networks based on dynamic tariff, reconfiguration, and re-profiling product, *IEEE Trans. Smart Grids*, 10(5), 4795-4805, 2019.

[52] Y. Liu, J. Li, and L. Wu, Coordinated optimal network reconfiguration and voltage regulator/der control for unbalanced distribution systems, *IEEE Trans. Smart Grids*, 10(3), 2912-2922, 2019.

[53] R. K. Mishra and K. S. Swarup, Adaptive weight-based self reconfiguration of smart distribution network with intelligent agents *IEEE Trans. on Emerging Topics in Computational Intelligence*, 2(6), 464-472, 2018.

[54] Berg, R., Hawkins, E. S., and Pleines, W. W. Mechanized calculation of unbalanced load flow on radial distribution circuits. *IEEE Trans. on power apparatus and systems*, (4), 415-421, 1967.

[55] Chen, T. H., Chen, M. S., Hwang, K. J., Kotas, P., and Chebli, E. A. Distribution system power flow analysis-a rigid approach. *IEEE Trans. Power Del.*, 6(3), 1146-1152, 1991.

[56] Lavorato, M., Franco, J. F., Rider, M. J., and Romero, R. Imposing radiality constraints in distribution system optimization problems. *IEEE Trans. Power Syst.*, 27(1), 172-180, 2011.

[57] Stevenson Jr, W. and Grainger, J. (1994). *Power system analysis*. McGraw-Hill Education.

[58] A. A. Heidari, S. Mirjalili, H. Faris, I. Aljarah, M. Mafarja, H. Chen, "Harris hawks optimization: Algorithm and applications", *Future Generation Computer Systems*, vol. 97, pp. 849-872, 2019.

[59] X.-S. Yang, T. Ting, and M. Karamanoglu, Random walks, Lévy flights, Markov chains and metaheuristic optimization, *Future information communication technology and applications*, ed: Springer, 1055–1064, 2013.
[60] Khodr, H. M., Olsina, F. G., De Oliveira-De Jesus, P. M., Yusta, J. M. "Maximum savings approach for location and sizing of capacitors in distribution systems". *Electric Power Systems Research*, 78(7), 1192-1203, 2008.
[61] Das, D., Kothari, D. P., Kalam, A. "Simple and efficient method for load flow solution of radial distribution networks", *Int J Electre Power Energy Syst*, 17(5), 335-46, 1995.
[62] M. E. Baran and F. F. Wu, "Optimal Capacitor Placement on Radial Distribution Systems," *IEEE Trans. Power Del.*, 4(1), 725-734, 1989.
[63] R. D. Zimmerman, C. E. Murillo-Sanchez, and R. J. Thomas, "MATPOWER: Steady-State Operations, Planning and Analysis Tools for Power Systems Research and Education," *IEEE Trans. Power Syst.*, 26(1), 12–19, 2011.
[64] De Jong, P., Sánchez, A.S., Esquerre, K., Kalid, R.D.A. and Torres, E.A., Solar and wind energy production in relation to the electricity load curve and hydroelectricity in the northeast region of Brazil. Renewable and Sustainable Energy Reviews, 23, 526-535, 2013.
[65] Shi, Q., Li, F., Olama, M., Dong, J., Xue, Y., Starke, M., Winstead, C. and Kuruganti, T. Network reconfiguration and distributed energy resource scheduling for improved distribution system resilience. *Int. J. Electr. Power Energy Syst.*, 124, 106355, 2021.
[66] H.M. Khodr, J. Martínez-Crespo, Z.A. Vale, and C. Ramos, "Optimal methodology for distribution systems reconfiguration based on OPF and solved by decomposition technique," *EUR T ELECTR POWER*, 20(6), 730-746, 2010.

Ahmed M. Helmi has received his B.Sc. (with honors) from Computer and Systems (CSE) Dept., Faculty of Engineering, Zagazig University in 2005. He has obtained M.Sc. and Ph.D in Computing from Computer Science (CS) Dept., Universitat Politècnica de Catalunya (UPC), Barcelona, Spain in 2010 and 2013, respectively. He did a short stay at Institute of Discrete Mathematics and Geometry, Technical University of Vienna, in 2012. He did a postdoctoral studies at CS dept. in UPC between 2019 and 2020. Since 2013, he is a lecturer at CSE Dept. in Zagazig University. He has published a number of research articles and book chapters in analysis of algorithms and stochastic optimization techniques. Recently, he is interested in research areas like human activity recognition, sensory data processing and applications of optimization techniques in engineering applications. Also, machine learning tools like artificial neural networks and convolutional neural networks are of his interests.

Raffaele Carli (M'17) received the Laurea degree in Electronic Engineering with honours in 2002 and the Ph.D. in Electrical and Information Engineering in 2016, both from Politecnico di Bari, Italy. From 2003 to 2004, he was a Reserve Officer with Italian Navy. From 2004 to 2012, he worked as System and Control Engineer and Technical Manager for a space and defense multinational company.

Dr. Carli is currently an Assistant Professor in Automatic Control at Politecnico di Bari, and his research interests include the formalization, simulation, and implementation of decision and control systems, as well as modeling and optimization of complex systems. He was member of the International Program Committee of 20+ international conferences and guest editor for special issues on international journals. He is author of 60+ printed international publications.

Mariagrazia Dotoli (M'96, SM'12) received the Laurea degree in Electronic Engineering with honours in 1995 and the Ph.D. in electrical engineering in 1999 from Politecnico di Bari (Italy).

She has been a visiting scholar at the Paris 6 University and at the Technical University of Denmark. She is expert evaluator of the European Commission since the 6th Framework Programme. She is a Full Professor in Automatic Control at Politecnico di Bari, which she joined in 1999. She has been the Vice Rector for research of Politecnico di Bari and a member elect of the Academic Senate. Her research interests include modeling, identification, management, control and diagnosis of discrete event systems, manufacturing systems, logistics systems, traffic networks, smart grids and networked systems.

Prof. Dotoli was co-chairman of the Training and Education Committee of ERUDIT, the European Commission network of excellence for fuzzy logic and uncertainty modeling in information technology, and was key node representative of EUNITE, the EUropean Network of excellence on Intelligent Technologies. She is a Senior Editor of the IEEE TRANS. ON AUTOMATION SCIENCE AND ENGINEERING and an Associate Editor of the IEEE TRANS. ON SYSTEMS, MAN, AND CYBERNETICS and of the IEEE TRANS. ON CONTROL SYSTEMS TECHNOLOGY. She is the General chair of the 29th Mediterranean Conference on Control and Automation. She was the Program co-chair of the 2020 and 2017 IEEE Conference on Automation Science and Engineering, the Workshop and Tutorial chair of the 2015 IEEE Conference on Automation Science and Engineering, the Special Session co-chair of the 2013 IEEE Conference on Emerging Technology and Factory Automation and chair of the National Committee of the 2009 IFAC Workshop on Dependable Control of Discrete Systems. She was member of the International Program Committee of 80+ international conferences. She is author of 200+ publications, including 1 textbook (in Italian) and 70+ international journal papers.

Haitham S. Ramadan obtained his PhD from the Dept. of Energy and Automatic Control of École Supérieure d' Électricité (SUPELEC), University of South Paris XI, France in March 2012. From June 2012 he has been a Lecturer in the Electrical Power and Machines Dept., Faculty of Engineering, Zagazig University, Egypt. Since August 2013 he did several postdoctoral research missions in the Laboratory of Signal and Systems (LSS), the Federation of Research of Fuel Cells and the University of Belfort Montbéliard in France. Since June 2017 Dr. Ramadan is an Associate Professor in the Power and Machines Dept., Faculty of Engineering, Zagazig University, Egypt.

He was the Co-chair of the annual International Conference of Emerging and Renewable Energy: Generation and Application (ICEREGA) since 2017, the General Secretary of ICREGA16, Guest and Managing Editor in different Elsevier journals, author of 80+ high-ranked journal and conference papers. In 2021 Dr. Ramadan joined the ISTHY (Institut international sur le Stockage de l'Hydrogéne) in France. He was/is the Principal Investigator and coordinator of several Egyptian-French projects and international collaborations, and summer schools. His fields of interest include hydrogen reservoirs and storage systems, power systems control and optimization, multi-physical modelling of energy systems, renewable energy (solar and wind), hybrid power systems, hydrogen economy and technologies, fuel cells and batteries, energy management topics, electric and hybrid electric vehicles, microgrids, smart grids and HVDC.